1-1-1999

Three-dimensional wind turbine simulation and analysis

Jennifer Ann Cordero
Iowa State University

Three-dimensional wind turbine simulation and analysis

by

Jennifer Ann Cordero

A thesis submitted to the graduate faculty

in partial fulfillment of the requirements for the degree of

MASTER OF SCIENCE

Major: Mechanical Engineering

Major Professors: R. Ganesh Rajagopalan and Robert C. Brown

Iowa State University

Ames, Iowa

1999

Graduate College
Iowa State University

This is to certify that the Master's thesis of

Jennifer Ann Cordero

has met the thesis requirements of Iowa State University

Signatures have been redacted for privacy

TABLE OF CONTENTS

LIST OF TABLES

LIST OF FIGURES

ABSTRACT

This research uses a new technique, three-dimensional computational fluid dynamics, to simulate and analyze wind turbine performance. A software package developed to do this, called Rot3dc, finds the numerical solution of the Navier-Stokes equations over the area of interest. In this code rotor blades are modeled as momentum sources. Several cases were run in this study to show the capabilities of the code. First a stand-alone rotor was modeled, followed by a turbine with nacelle and tower. Then this complete turbine was positioned at the center of small and large sloping terrains. Finally, the complete turbine was modeled off-center on a large sloping terrain.

The output generated by Rot3dc includes blade element data, such as angle of attack, lift, drag, torque, thrust, and velocity and coefficient of performance. The flow field solution can also be visualized in a software package called FAST, Flow Analysis Software Toolkit.

The Rot3dc output is compared to that of WT_Perf, a traditional computer code currently used by the wind power industry. This code is not designed to directly model the influence of turbine components, such as the nacelle and tower, on the flow. In addition, it does not have the capability to include the interactions of terrain on the flow.

Rot3dc showed to provide more information about the system. Analyses were performed to determine the variation of loading along the length of the blade at different wind speeds, the cyclic variation of load as the blade rotates, especially due to the tower wake, and loading at particular stations of the blade at different azimuth angles. In this study, the CFD method showed variations between the different turbine configurations, evidence that it can model turbines in a more realistic environment than with traditional methods.

Results show that this method can have a significant impact on the wind turbine industry.

Information provided by this technique can be used to minimize vibrations and variational loading that cause stress and fatigue. This capability will ultimately extend the life of the blades, reduce the overall cost of the turbine and help make wind power more competitive with traditional forms of energy.

CHAPTER 1. INTRODUCTION

The rotation of the earth and the temperature gradients across the earth's surface due to the spherical shape of the earth cause winds to flow across the globe. This wind resource has been exploited by humans since the thirteenth century for a myriad of uses, such as pumping water and generating electricity. In the past, stand-alone windmills were able to provide electricity and water to remote locations. In recent years, particularly during the oil crisis of the 1970s, these windmills have been engineered to maximize their performance and output. Their uses have also been expanded from stand-alone applications to utility-scale operations where fields of turbines have been connected to provide power to cities. These applications provide a clean alternative to fossil-fuel energy sources.

The wind turbine that is currently the most widely used is the horizontal axis wind turbine (HAWT). This device consists of a rotor, often with two or more rotating blades, a hub to which the blades are connected, a nacelle, which houses the electrical generator and other components, and a tower.

Engineers have conducted analyses on a variety of wind turbines in order to improve performance and maximum output. The traditional analyses are based on actual data collected from either wind tunnel experiments or experimental wind turbine installations. More recently, scientists have developed computer programs to simulate wind turbine performance. These programs are currently used by industry today. However, these codes have serious limitations. Some of these limitations include the inability to simulate the interference of the tower and nacelle on the flow and the inability to model a turbine in a realistic environment, such as on a sloping terrain. Furthermore, the field data often does not compare well with the output of these codes. Apparently, a more sophisticated and accurate approach is needed.

A more modern approach includes using three dimensional computational fluid dynamics (CFD) to simulate a flow field. A new commercial software package called Rot3dc has been developed to accomplish this goal.

The goal of this research is to model, simulate, and analyze various HAWT arrangements using Rot3dc and to compare this approach to more traditional approaches. The traditional approach discussed in this research is the use of a computer code called WT_Perf developed at the National Renewable Energy Laboratory. This research will show that Rot3dc provides more flexibility and produces more accurate information than WT_Perf, information that can be used in more advanced design of wind turbines and wind farms.

This comparison can have a significant impact on the wind turbine industry. The CFD method has the capability to model the influence of solid bodies on the flow directly. Modeling the effects of solid bodies directly allows researchers to analyze the cyclic variation of load on the blades caused by the tower and terrain, the vibration and noise caused by the bodies interfering with the flow, as well as other characteristics. These characteristics are known to result in fatigue and shorten the life of rotor blades. Analysis of these behaviors can help to improve the performance of wind turbine blades, ultimately lowering the overall cost. Reducing the cost of the blades will help to make wind power more cost effective and competitive with other, less environmentally-friendly, forms of power.

CHAPTER 2. BACKGROUND THEORY

2.1 The Wind Resource

Certain factors affect the wind resource, namely location, elevation above ground level, and season. Several regions across the globe experience strong, frequent winds. In fact, the World Energy Council estimates that 27% of the earth's land surface experiences annual average wind speeds higher than 5.1 m/s at 10 m above the surface. While only 4% of this area might actually be available for wind farms, this would amount to 20,000 TWh per year, almost double the total world electricity consumption (Walker and Jenkins 15).

The wind speed at the surface of the earth is zero because of the friction between the air and the ground's surface (Walker and Jenkins 6). The wind speed increases with height until about 2 km above ground, when the change in wind speed becomes negligibly small. At higher elevations, the wind blows steadier and with fewer interruptions than at ground level. The vertical variation of wind speed, or the wind speed profile, can be described by several functions. One of these functions is the power exponent function:

$$V(z) = V_r \left(\frac{z}{z_r}\right)^{\alpha} \tag{2.1}$$

where z is the height above ground level, V_r is the wind speed at the reference height z_r above ground level, V(z) is the wind speed at height z, and α is an exponent which depends on the roughness of the terrain (Walker and Jenkins 7). This function can be used to determine the mean wind velocity at a certain height if the mean wind velocity is known at a reference height (Walker and Jenkins 8). Seasonal variations can be seen in the wind resource. Spring normally experiences the highest wind velocities (Elliott 54).

In describing the wind resource, statistical representations must be made since no direct

mathematical function can adequately characterize it. The parameters which are used to describe the wind resource are wind power density and the wind speed frequency distribution. Wind power density is the mass flow rate of an airstream flowing through an area A, ρAV, multiplied by the kinetic energy in a flow of air through a unit area perpendicular to the wind direction, $\frac{1}{2}V^2$. It is given by:

$$P_w = (\rho AV)\frac{1}{2}V^2 = \frac{\rho AV^3}{2} \tag{2.2}$$

where ρ is the air density and V is the wind velocity. The wind speed distribution, or the frequency the site experiences certain velocities, is given by:

$$f(V) = \left(\frac{k}{c}\right)\left(\frac{V}{c}\right)^{k-1} exp\left[-\left(\frac{V}{c}\right)^{k}\right] \tag{2.3}$$

The frequency distribution is based on the Weibull function where k is the shape parameter and describes the variability of the regime, and c is the velocity scale parameter (Walker and Jenkins 9). For k close to 1, the regime experiences highly variable winds, while for k above 2, the regime receives more constant winds (Cavallo et al. 126). These parameters can change from season to season, resulting in different frequency distributions. Only a portion of the wind power density is available for useful work. The maximum power that can be extracted from a wind stream is $\frac{16}{27}$ x P_w = 0.593 x P_w, or 59%. This quantity is referred to as the Betz limit (Cavallo et al. 124).

In practice, only a much smaller fraction of power can be extracted from a wind stream by a wind turbine. This fraction is denoted by C_p, the turbine's coefficient of performance. C_p is a function of the wind velocity, angular velocity of the rotor, ω, the pitch angle, β, the airfoil shape, and the number of blades, among other parameters. Thus, the output power of a wind turbine is:

$$P_{out} = C_p\frac{\rho AV^3}{2} \tag{2.4}$$

An airfoil has optimum values of lift and drag for one angle of attack, α, or for one value of relative wind speed; therefore, C_p for a wind turbine with fixed blades and operating at a fixed angular velocity will also have a maximum value that decreases at higher or lower wind speeds (Cavallo et al. 130).

2.2 Turbine Components

The modern HAWT consists of six sub-systems: the rotor, the drive train, the yaw system, electrical systems, the tower, and balance-of-station systems. The rotor converts the wind's kinetic energy into kinetic energy of rotation. In general, a rotor consists of one, two, or three blades mounted on a hub. Rotors can either be rigid or teetered. In a teetered rotor, the plane of rotor rotation can vary a few degrees from the perpendicular to the average wind velocity. Both rigid and teetered rotors can have either fixed (stall-controlled) or variable pitch. This parameter limits the maximum turbine output by setting the cutoff speed of the turbine, and controls the amount of energy length, altering the pitch angle and the lift and drag forces on the blades. Their flexibility allows them to capture more wind energy at higher wind speeds than fixed pitch rotors. Fixed (stall-controlled) pitch rotors are less complex; however, they lose lift at high wind speeds, thus limiting the maximum amount of energy captured.

The drive train consists of low- and high-speed shafts, the mechanical braking system, bearings, couplings, gearbox, or transmission, and the nacelle. The gears of the drive train increase the angular velocity of the rotor from 0.5 to 2 hertz (30-120 rpm) to the output shaft rotational speed of 20 to 30 hertz (1200 to 1800 rpm). This higher speed is required by generators producing power at 50 to 60 hertz. The nacelle is the structure containing these devices, protecting them from the elements. The yaw control system is responsible for aligning the rotor perpendicular to the wind stream and can be either passive or active depending on which direction the turbine is designed to capture wind energy: up-wind or down-wind. Down-wind machines use a passive yaw control system, similar to the weather-vane-like effect in positioning the rotor, while up-wind machines use an active yaw system. This system requires a drivetrain that is activated by a change in wind direction. Modern wind turbine electrical systems are designed with induction generators. Additional electrical equipment includes low-maintenance electronic controls and sensors.

Lastly, the balance-of-station systems include roads, ground-support equipment, and inter-connection equipment. The land area required for this subsystem is approximately 1% of the entire wind turbine plant area (Cavallo et al. 136-140).

2.3 Turbine Operational Characteristics

The transfer of wind power to electrical power depends on wind turbine type–variable pitch or stall controlled–and turbine rating (maximum power output). The electrical energy output from a wind turbine is a function of the wind velocity at the hub height. A power curve can be developed to show the energy output at each wind speed. The power curve indicates the following parameters:

- Cut-in wind speed V_i: the wind speed at which the turbine starts to produce net power; this is higher than required to start the blades rotating

- Cut-out wind speed V_o: to reduce mechanical loads on the turbine, it is stopped at wind speeds above the cut-out wind speed

- Rated power P_r: the nominal maximum continuous power output of the wind turbine at the output terminals of the generator (net of losses)

- Rated wind speed V_r: the wind speed at which rated power is produced

As the wind speed increases, the power curve approaches the rated power. Ideally, the power remains constant at the rated power until the cut-out speed is reached (Walker and Jenkins 52-55). In Figure 2.1, the cut-out speed would be 25 m/s. At this point, the turbine would shut down and the power output would return to zero.

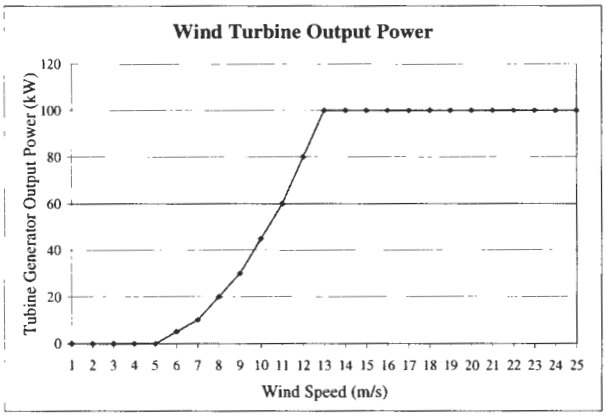

Figure 2.1 Wind Turbine Power Curve

The average electrical output power of a turbine is determined by:

$$P_{avg} = \int P_{out}(V) \cdot f(V)\, dV \tag{2.5}$$

where $P_{out}(V)$ is the power output of the turbine as a function of wind velocity, which depends on the physical design of the turbine. As discussed in section 2.1, $f(V)$ is the wind speed distribution. If $P_{out}(V)$ is written as $P_r \cdot \mathrm{g(V)}$, then:

$$P_{avg} = P_r \cdot \int g(V) \cdot f(V)\, dV \tag{2.6}$$

where the integral is the ratio of annual average power output to the rated power of the turbine, otherwise known as the capacity factor, CF. More briefly, $CF = P_{avg}/P_r$ (Cavallo et al. 132).

2.4 Wind Turbine Aerodynamics

The aerodynamic forces exerted upon a wind turbine rotor are explained by classic airfoil theory. When the airfoil moves in a flow, a pressure distribution occurs around it. This distribution is based on the angle of incidence, the angle between the airfoil chord and the direction of the flow. On the upper side of the airfoil there is a negative pressure, and on the lower side, there is a positive pressure. Loads are exerted on the airfoil due to the pressure distribution. These loads include two forces, lift and drag, and one torque, the pitching moment. Lift, L, is perpendicular to the direction of the flow, V. The drag, D, is parallel to the flow and perpendicular to the lift. The pitching moment, M, is given relative to a specific point, usually at 0.25 of the chord. These forces are typically expressed as dimensionless aerodynamic coefficients of the airfoil:

$$C_L = \frac{L}{\frac{1}{2}\rho A V^2} \tag{2.7}$$

$$C_D = \frac{D}{\frac{1}{2}\rho A V^2} \tag{2.8}$$

$$C_M = \frac{M}{\frac{1}{2}\rho c A V^2} \tag{2.9}$$

where ρ and V are the air density and wind speed, and A and c are the plan area and chord length of the airfoil. In a wind turbine rotor, the lift and drag forces on the blades are transformed into a rotational torque and axial thrust force. The torque produces useful work by turning the shaft of the generator, whereas the thrust works to overturn the turbine and must be resisted by the tower and the foundations.

The magnitude of the lift and drag forces depends on the airfoil characteristics, the relative wind speed, and the angle the relative wind makes with the chord line of the airfoil, or the angle of attack. The relative wind speed depends on the rotational speed of the blade and the wind speed. The drag force is parallel to the relative wind, and the lift force is perpendicular. Once the lift and drag forces are resolved parallel and perpendicular to the direction of rotation of the blade element, one can see that the lift force creates useful torque while the drag force opposes it. Both the lift and drag forces contribute to the axial thrust force on the rotor. The total useful torque developed by the rotor is the sum of the torques developed by each blade element; the same is true for the thrust force. A high ratio of lift coefficient to drag coefficient is needed for a high efficiency rotor. A diagram of these forces is shown in Figure 2.2 (Walker and Jenkins 23-27).

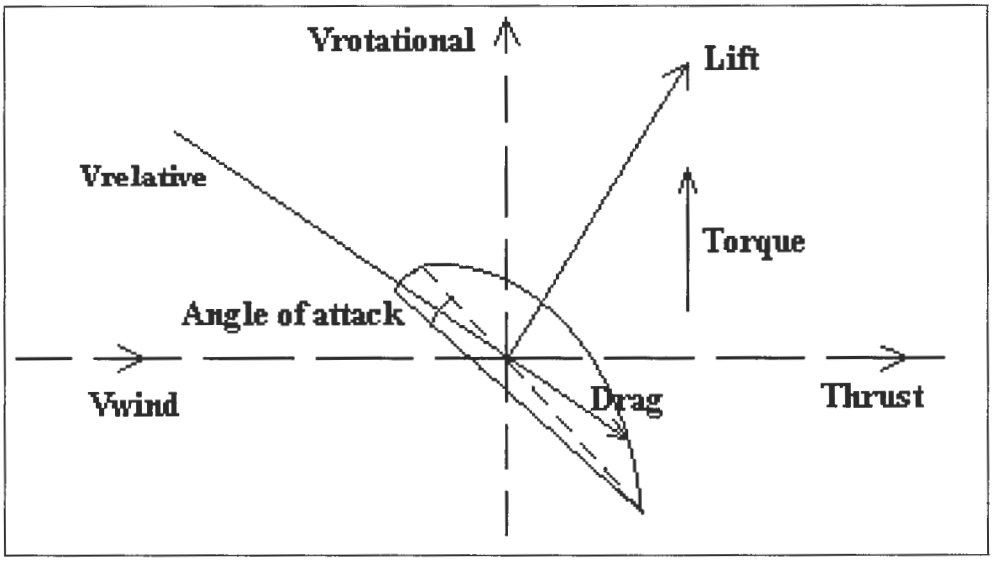

Figure 2.2 Forces on a Blade Element

The tip speed ratio, λ, of a rotor is

$$\lambda = \frac{V_{tip}}{V_{wind}} = \frac{\omega R}{V_\infty} \tag{2.10}$$

where R is the rotor radius, ω is the rotational speed in radians/second, and V_∞ is the freestream wind speed (Walker and Jenkins 22). Output power was discussed earlier as the wind power density multiplied by the coefficient of performance. It can also be denoted by P_{out} = torque * rotor speed. This formulation is used for the computations discussed in this paper.

CHAPTER 3. THREE DIMENSIONAL SIMULATION

3.1 Introduction

The aim of this research is to model a wind turbine in a realistic environment using three dimensional computational fluid dynamics (CFD) analysis. Rot3dc is a CFD software package developed by Sukra Helitek, Inc. that has the capability to simulate performance of applications such as helicopter blades and wind turbines. This research will show that Rot3dc provides a greater flexibility in analyzing rotor performance compared to more traditional methods. Like all other CFD methods, this program finds a numerical solution of the governing equations over the area of interest, called the computational domain. To use Rot3dc, the user must specify certain parameters for modeling. Then, when the program is run, it generates a variety of output data that can be used to conduct blade element and performance analyses.

3.2 Flow Field Modeling

The blades of the turbine are modeled as momentum sources in the equations that govern the flow. The flow is assumed to have constant density and viscosity, and the flow field is determined by solving the mass and momentum conservation equations, the Navier-Stokes equations. The unsteady, incompressible, laminar Navier-Stokes equations are:

continuity:

$$\frac{\partial \rho}{\partial t} + \frac{\partial u}{\partial x} + \frac{\partial v}{\partial y} + \frac{\partial w}{\partial z} = 0 \tag{3.1}$$

x-momentum:

$$\frac{\rho \partial u}{\partial t} + \rho \left(u\frac{\partial u}{\partial x} + v\frac{\partial u}{\partial y} + w\frac{\partial u}{\partial z} \right) = \mu \left(\frac{\partial^2 u}{\partial x^2} + \frac{\partial^2 u}{\partial y^2} + \frac{\partial^2 u}{\partial z^2} \right) - \frac{\partial p}{\partial x} + S'_x \tag{3.2}$$

y-momentum:

$$\frac{\rho\partial v}{\partial t} + \rho\left(u\frac{\partial v}{\partial x} + v\frac{\partial v}{\partial y} + w\frac{\partial v}{\partial z}\right) = \mu\left(\frac{\partial^2 v}{\partial x^2} + \frac{\partial^2 v}{\partial y^2} + \frac{\partial^2 v}{\partial z^2}\right) - \frac{\partial p}{\partial y} + S'_y \tag{3.3}$$

z-momentum:

$$\frac{\rho\partial w}{\partial t} + \rho\left(u\frac{\partial w}{\partial x} + v\frac{\partial w}{\partial y} + w\frac{\partial w}{\partial z}\right) = \mu\left(\frac{\partial^2 w}{\partial x^2} + \frac{\partial^2 w}{\partial y^2} + \frac{\partial^2 w}{\partial z^2}\right) - \frac{\partial p}{\partial z} + S'_z \tag{3.4}$$

where μ is the flow viscosity and S'_x, S'_y, and S'_z are the time averaged source terms per unit volume due to the turbine's motion in the coordinate directions x, y, and z respectively. These source terms represent the rotor-induced force per unit volume at a point. Through these terms, the rotor's influence is introduced into the flow field. Thus, the rotor is modeled by a series of momentum sources occurring in a specific region of the domain (Rajagopalan and Mathur 16).

The numerical procedure for solving the governing equations is based on Patankar's SIMPLER algorithm, which uses a finite-volume based method. More information about this algorithm can be found in Patankar. The iterative procedure for solving the problem is shown in Figure 3.1. The left branch shows the steps in the momentum-source calculations, while the right branch lists the procedure in the SIMPLER algorithm. The two are connected through the velocity field which is used to determine the rotor force. The iterations are continued until convergence. The forces on the blades can then be calculated in the same manner as the source terms (Mathur 35-36).

3.3 Rotor Modeling

Before determing the rotor's influence on the flow field, one must find the locations where that influence is felt. Once this is accomplished, one may calculate the momentum equation source terms at these locations. These steps require a description of the rotor geometry, which can be provided with respect to several different coordinate systems and the transformations between them (Rajagopalan and Mathur 16).

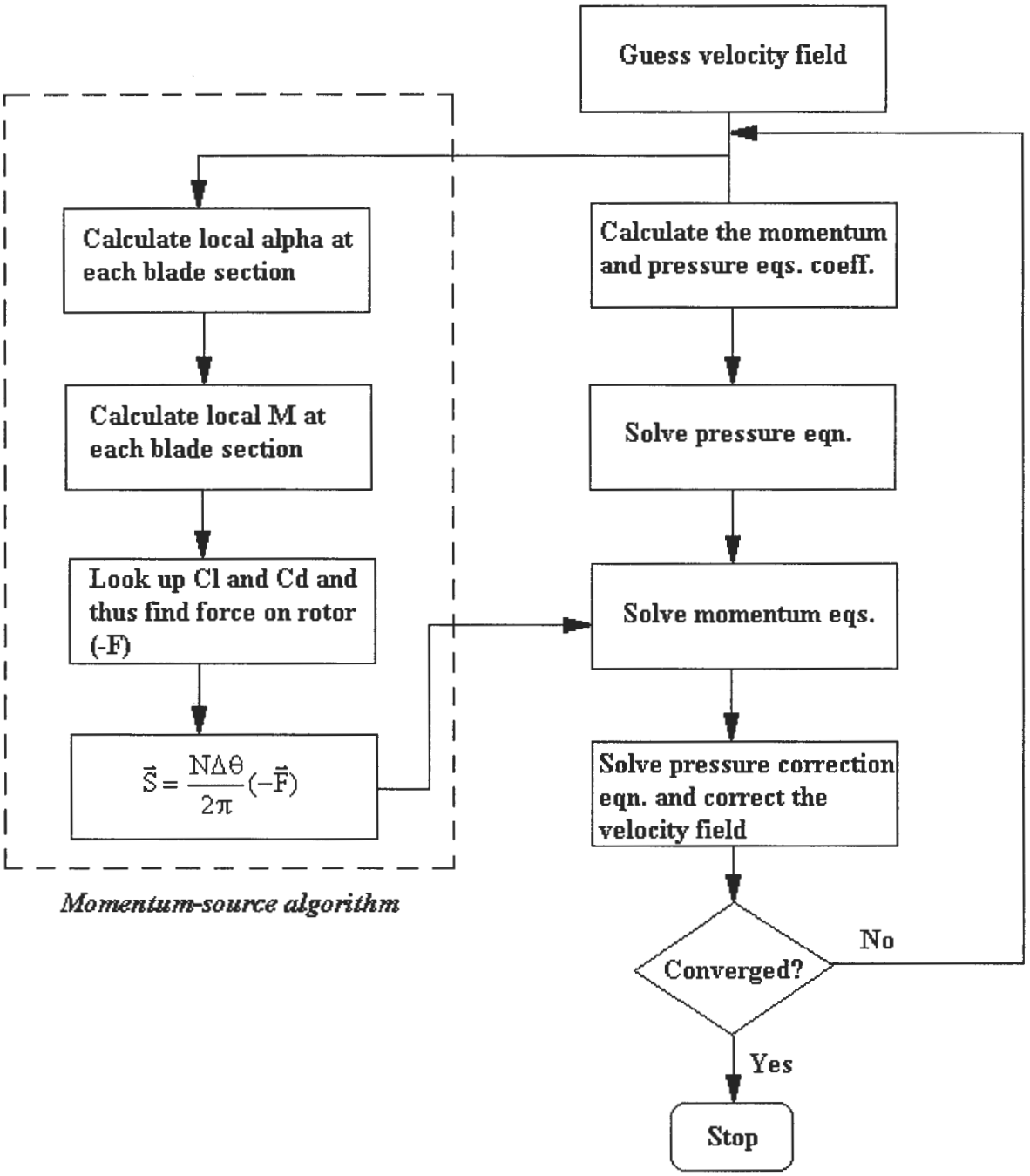

Figure 3.1 Iterative Solution Procedure

3.3.1 Coordinate System

The governing equations are solved in the computational domain, a rectangular body surrounding the rotor (described in more detail below). Cartesian coordinates (X, Y, Z) and the unit vectors $\hat{I}$, $\hat{J}$, and $\hat{K}$ describe this domain. The center of the rotor can be denoted by (X_c, Y_c, Z_C) with respect to this system. The rotor's axis of rotation is along the vector $\vec{\Omega}$ where

$$\vec{\Omega} = \Omega_1 \hat{I} + \Omega_2 \hat{J} + \Omega_3 \hat{K} \tag{3.5}$$

and $|\vec{\Omega}| = \Omega$, the rotational speed in radians per second (Rajagopalan and Mathur 16).

It is convenient to have the computational coordinates in the direction parallel and normal to the freestream velocity. For this study, the rotor was oriented in this manner, so no transformations were needed. The system was easily modeled with a simple translation from the local, rotor-based coordinate system to the global, computational domain-based coordinate system.

3.3.2 Rotor Discretization

The rotor blades are divided into elements along the length of the blade by circles drawn from the center of the rotor. The center of each blade segment describes a circle as it makes one complete revolution. Blade properties, such as chord length, twist, thickness, out of plane deflection, and the cross-sectional characteristics at the center of each element, are maintained throughout that element (Rajagopalan and Mathur 17).

3.3.3 Calculation of Rotor Forces

Let the fluid velocity at any point s on a blade be

$$\vec{V} = u\hat{I} + v\hat{J} + w\hat{K}. \tag{3.6}$$

The blade has velocity due to its rotation, $\vec{V_{bl}}$. Thus, the flow velocity relative to the blade is given by

$$\vec{V_{rel}} = \vec{V} - \vec{V_{bl}}. \tag{3.7}$$

From the components of relative velocity experienced by the airfoil and the angle of attack, one can find the aerodynamic force coefficients C_l and C_d for the section from the airfoil

characteristics (Rajagopalan 18). The lift and drag forces can then be found. The resultant aerodynamic force on the blade segment, $\vec{F}$ can be computed. The instantaneous force acting on the fluid element is then $-\vec{F}$. The time-averaged source terms $\vec{S} = (S_X, S_Y, S_Z)$ to be added to the discretized momentum conservation equations at this control volume are given by

$$\vec{S} = \left(\frac{N\Delta\theta}{2\pi}(-\vec{F})\right) \tag{3.8}$$

where N is the number of blades and $\Delta\theta$ is the angular distance through which the blade traverses in passing through the control volume (Rajagopalan 18).

3.4 Computational Domain

The wind turbine being studied is located at the center of the computational domain, a rectangular parallelopiped. The computational domain is specified by a grid system. This grid system consists of a three-block arrangement, which are designated as Block #1, Block #2, and Block #3, as given in Figure 3.2. Block #1 spans from the west-south-bottom corner of the computational domain to the corner of Block #2. Block #3 spans from the corner of Block #2 to the east-north-top corner of the computational domain. The turbine is located in Block #2. Each block is divided into several layers, however the layers in Block #2 are more complex since it contains the bodies. Block #2, the grid including the turbine, is called the body grid, and the grids upstream and downstream of the turbine are called the layer grids, as shown in Figure 3.3. (X, Y, Z) are the Cartesian coordinates of this domain, and (I, J, K) are the unit vectors in this coordinate system. The center of the rotor is located at (X_c, Y_c, Z_c) with respect to this system (Sukra Helitek 21-22). If the user wants the bodies to be located on the ground, as in this research, the height of Block #1 is reduced to zero and a no-slip boundary wall is introduced in the X-Y plane. If the user wants the bodies to be located in the freestream, then Block #1 will have some height.

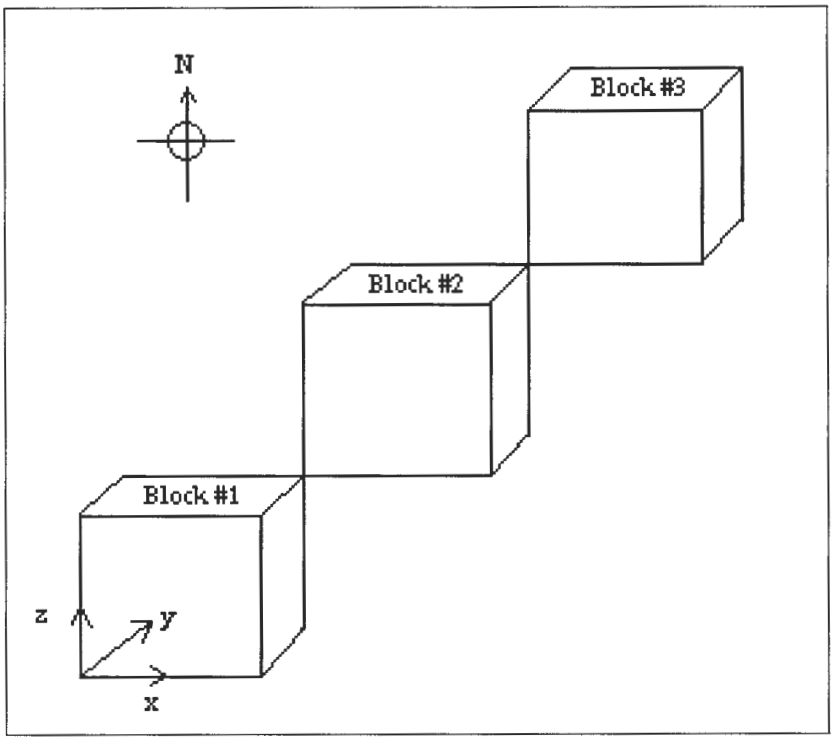

Figure 3.2 Three-block Computational Domain

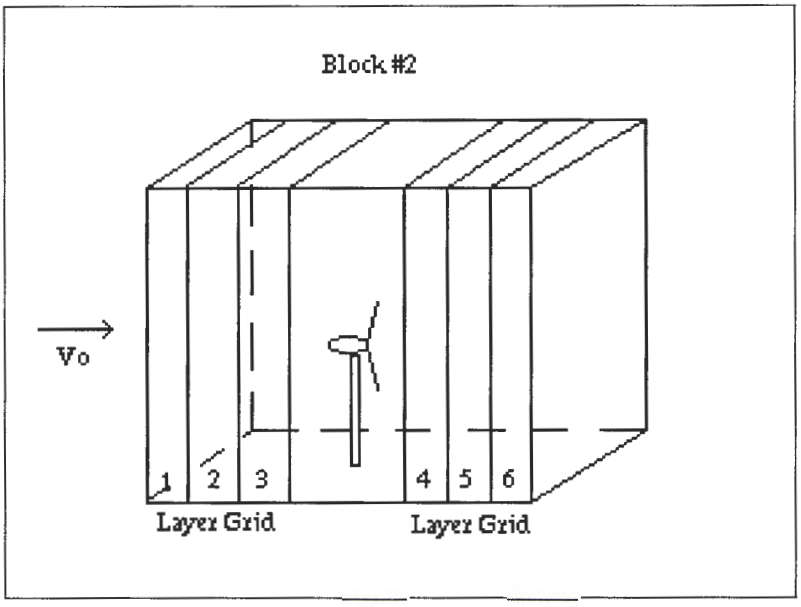

Figure 3.3 Block #2 Grid Specification

3.5 Output Generated

After the program is run, it generates several output files that provide the user with blade element data and performance data. The blade element files contain the following information: angle of attack, coefficient of lift, coefficient of drag, thrust, torque force, and twist at each radius and azimuth location. Rotor torque and thrust are also calculated. The coefficient of performance (C_p) can be derived from C_Q provided in the performance output files from the following equation:

$$C_p = C_Q \left(\frac{V_{tip}}{V_{wind}} \right)^3. \tag{3.9}$$

CHAPTER 4. RESULTS AND DISCUSSION

4.1 Introduction

The objective of this research is to model and simulate flow through a horizontal axis wind turbine using three dimensional CFD analysis. This chapter discusses the various cases that were generated and analyzes the output. Ultimately, Rot3dc, the CFD code that was used in this approach, will prove to be a flexible and accurate tool in the design and analysis of wind turbines for industrial and scientific use.

4.2 Rotor Description

This project simulated a down-wind horizontal axis wind turbine (HAWT). The parameters relating to the HAWT rotor included the number of blades, rotation direction, rotor radius, hub radius, tip speed, twist, cone angle, and number of locations on the radius and azimuth at which performance is to be monitored. Twist is the angle through which the blade is twisted from base to tip, and the cone angle is the angle the blades make from the rotor plane. This particular HAWT had two blades that rotated in a counter-clockwise direction, as seen when facing the turbine from the front. The radius of the rotor was 43 feet, and the hub radius was 3.52 feet. Tip speed was approximately 256.67 feet/second, and the cone angle was 7.0 degrees. For measurement, there were 100 locations on the radius and 24 locations on the azimuth. Neither flapping nor cyclic pitch was considered in this case. Table 4.1 shows the values for chord and twist along the length of the rotor blade. The c81 airfoil table was used in this analysis.

Table 4.1 AWT-26 Rotor Data

r/R	chord/R	twist (deg)
0.081761006	0.0642	5.8480
0.0970	0.0676	5.7060
0.1395	0.0738	5.4520
0.1500	0.0754	5.3930
0.2500	0.0860	4.8250
0.3500	0.0872	4.0080
0.4500	0.0816	2.8790
0.5500	0.0756	1.7620
0.6500	0.0686	0.8190
0.7500	0.0600	0.2540
0.8500	0.0500	0.0760
0.9500	0.0370	0.0270
1.0000	0.0282	0.0000

4.3 Boundary Conditions

Upstream of the turbine, at the inlet to the computational domain, the flow is uniform. A no-slip condition is imposed on the ground plane. Freestream conditions occur at the top of the computational domain. Downstream of the turbine, at the outlet of the computational domain, values are extrapolated from the interior grid points and are adjusted to conserve mass flow through the computational domain. Where included, the nacelle, tower, and terrain are modeled as solid bodies with all the components of the velocity set to and maintained as zero (Rajagopalan et al. 189).

4.4 Flow Field Conditions

The flow field characteristics shown in Table 4.2 were used in the analysis.

Table 4.2 Flow Field Conditions

Density (lb/ft^3)	0.00237
Temperature (R)	419
Gas Constant (ft-lb/slugs-R)	1718
Specific Heat Ratio	1.4
Viscosity (lb/ft-s)	3.719×10^{-7}
Pressure (lb/ft^2)	2116

4.5 Description and Analysis of Test Cases

Several cases were run in order to test the capability of Rot3dc to simulate a variety of environments. Each case is presented below.

4.5.1 Rot3dc Case 1: Single turbine rotor without nacelle or tower

In this case, a stand-alone rotor was simulated to represent the most idealistic scenario. This case was run for wind speeds of 10, 15, 20, 25, and 30 feet per second. The blade element results are shown for an azimuth angle of 90 degrees in Figures 4.1 to 4.11. The 90 degree azimuth angle is to the left of the turbine when facing the turbine from the front.

Figure 4.1 shows the various angles of attack for each wind speed. As can be expected, the angle of attack increases as wind speed increases, and it decreases along the length of the blade, dropping to zero at the tip. Ideally, a wind turbine designer would like the angle of attack to be constant along the length of the blade. The variation from root to tip causes stress on the blade, resulting in fatigue. This analysis provides the designer with information that can be used to minimize this variation.

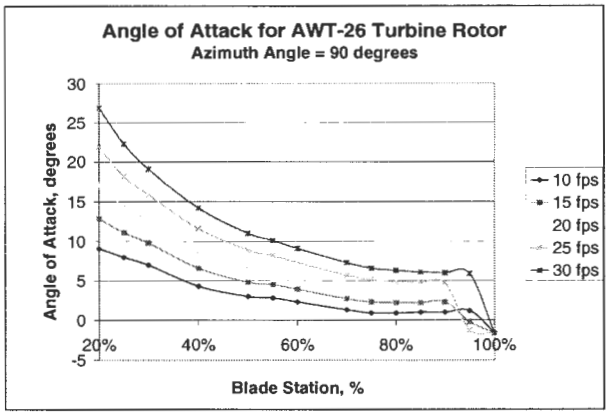

Figure 4.1 Angle of Attack for Rot3dc Case 1

Figure 4.2 shows the lift profiles for each wind speed. With increased wind speed, the lift increases. It decreases to zero at the tip. Drag is also an important parameter to analyze. It is the force that reduces the power output from the rotor; thus, it should be minimized. Figure 4.3 demonstrates the significant increase in drag with each incremental increase in wind speed. Furthermore, drag is felt primarily within the first half of the blade, decreasing drastically past the midpoint. This sharp contrast in drag force along the length of the blade can result in stress and even bending in the blade.

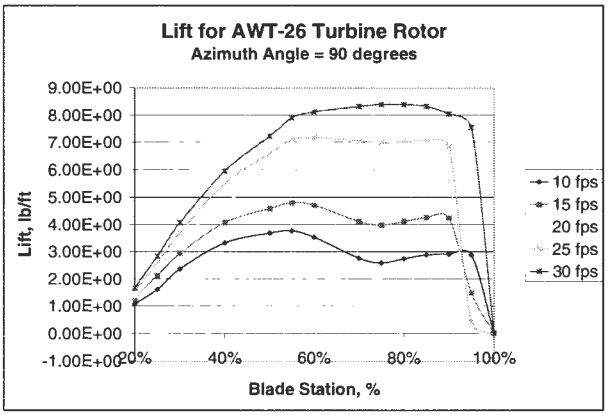

Figure 4.2 Lift for Rot3dc Case 1

In Figure 4.4, one can see the load profile for each wind speed. Load is the resultant component of lift and drag in the direction normal to the rotor disk. Similar to the lift profile, the load increases with wind speed, and decreases to zero at the blade tip.

Thrust is shown in Figure 4.5. Due to sign conventions, thrust is negative; however, the shape of the graph is similar to the lift and the load. Torque force is shown in Figure 4.6. Similar to thrust, the sign convention makes the values negative. The torque force decreases with increases in wind speed.

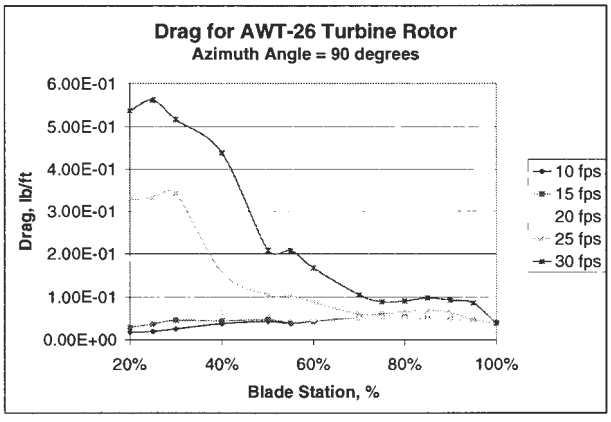

Figure 4.3 Drag for Rot3dc Case 1

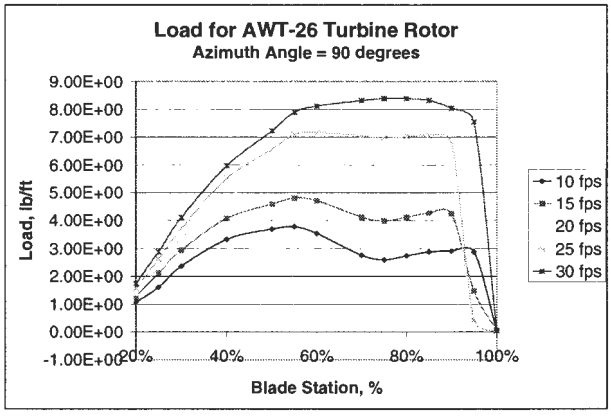

Figure 4.4 Load for Rot3dc Case 1

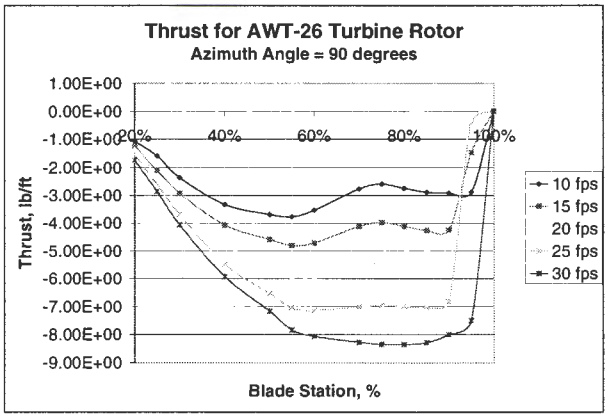

Figure 4.5 Thrust for Rot3dc Case 1

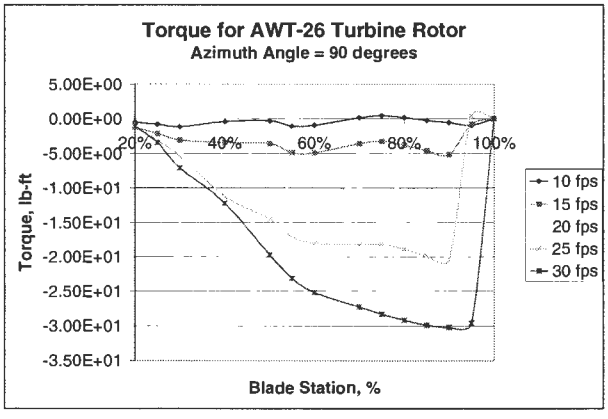

Figure 4.6 Torque Force for Rot3dc Case 1

Figures 4.7 and 4.8 show the lift and drag coefficients for the turbine rotor. They coincide well with the lift and drag charts discussed earlier. The radial velocity, shown in Figure 4.9, is the outward velocity of the wind as it passes through the rotor blades. Unlike some of the other blade element characteristics, it does not change significantly as the wind speed is varied.

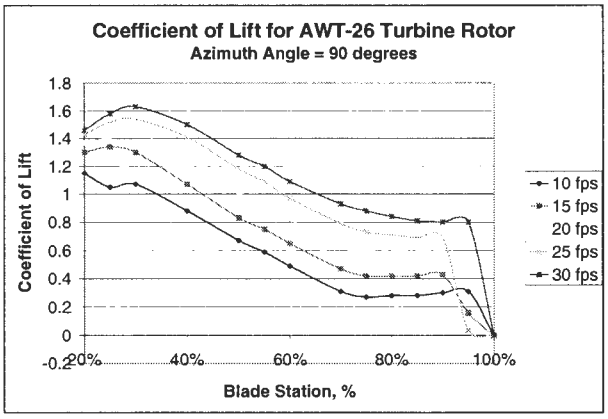

Figure 4.7 Lift Coefficient for Rot3dc Case 1

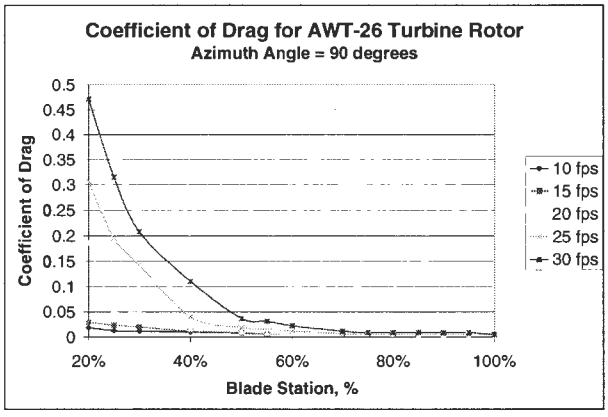

Figure 4.8 Drag Coefficient for Rot3dc Case 1

Figure 4.10 shows the angular velocity of the flow as it passes through the wind turbine rotor. This characteristic is also known as swirl. Note the distinguishing shape: the flow expe-riences the greatest swirl near the center of the rotor, and decreases to zero at approximately the midpoint of the blade.

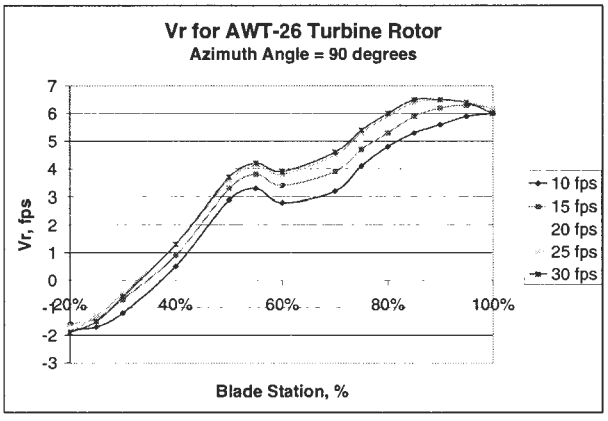

Figure 4.9 Radial Velocity for Rot3dc Case 1

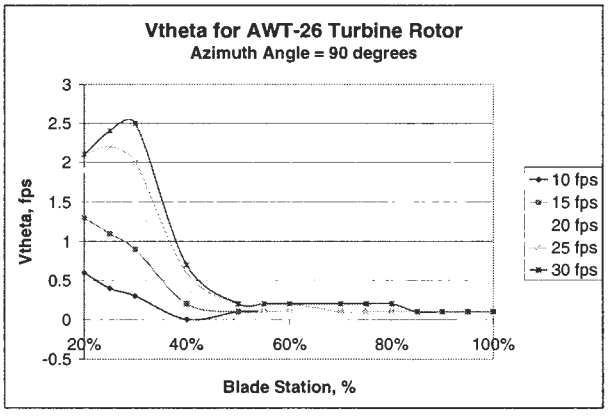

Figure 4.10 Angular Velocity for Rot3dc Case 1

Figure 4.11 shows the velocity of the wind stream perpendicular to the plane of the rotor as it passes through the wind turbine. A vast majority of the wind stream remains flowing in this direction, and only a small fraction is displaced in the radial or angular directions.

All of the parameters discussed above, angle of attack, lift, drag, thrust, torque, and velocity, are extremely useful to the wind turbine designer. This information can help in the design of wind turbines so that variation along the blade and at various wind speeds is reduced, extending the life of the blades.

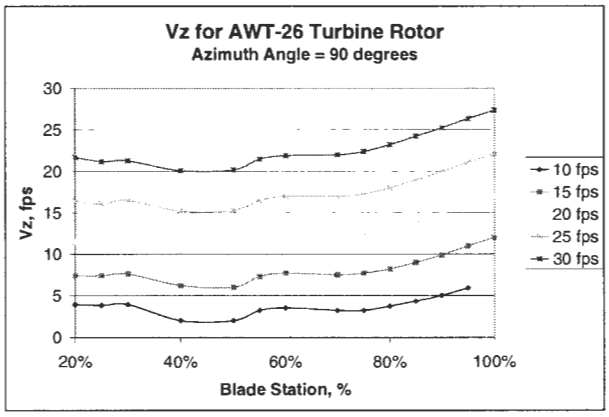

Figure 4.11 Axial Velocity for Rot3dc Case 1

4.5.2 Rot3dc Case 2: Single turbine with nacelle and tower

For this case, a nacelle and tower were added to the rotor described in the previous section. The nacelle was modeled as a rectangular box with a length of 10 feet and a height and width of 6 feet each. The tower was modeled as a cylindrical tube with a height of 86.25 feet and a diameter of 6 feet. The turbine was modeled on a flat terrain for the same wind speeds as above. The results are presented for and azimuth angle of 90 degrees in Figures 4.12 to 4.22.

The angles of attack for case 2 are presented in Figure 4.12. Similar to case 1, they increase as wind speed increases. However, the addition of the nacelle and tower have caused the angle of attack to increase by a few degrees for each wind speed.

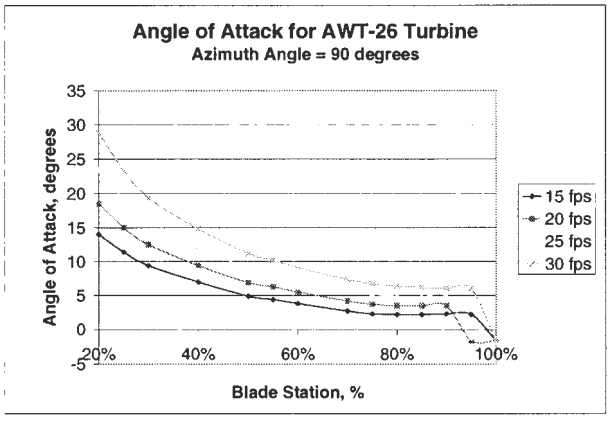

Figure 4.12 Angle of Attack for Rot3dc Case 2

Figures 4.13 and 4.14 illustrate the lift and load for case 2. The profiles have similar shape and values to those illustrated for case 1. Drag for case 2 is shown in Figure 4.15. It is significantly higher in this case, compared to case 1. Apparently, the nacelle and tower add to the drag experienced by the rotor blades.

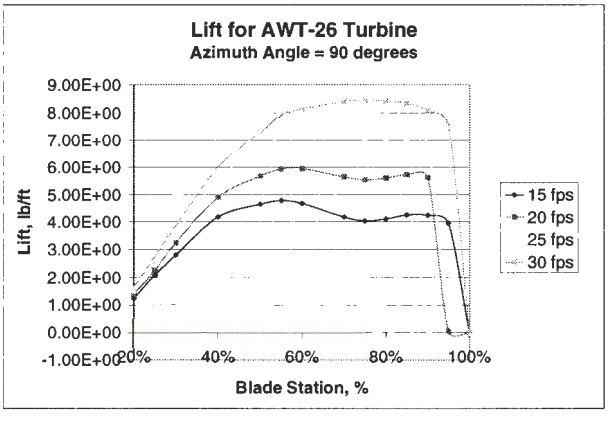

Figure 4.13 Lift for Rot3dc Case 2

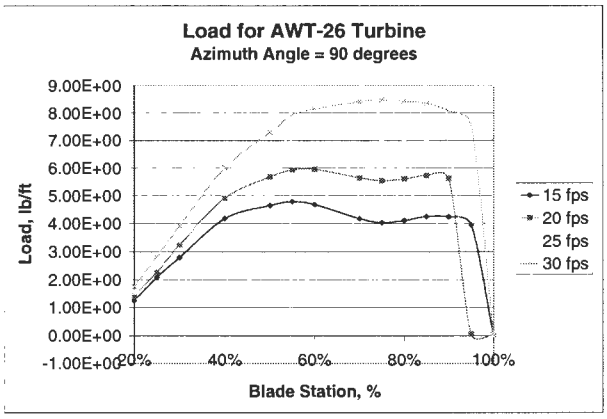

Figure 4.14 Load for Rot3dc Case 2

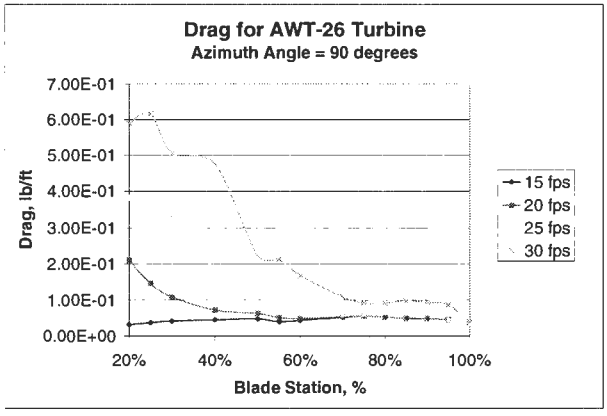

Figure 4.15 Drag for Rot3dc Case 2

Figures 4.16 and 4.17 show the thrust and torque force for case 2. Virtually no change can be seen for these characteristics between cases 1 and 2. The lift coefficient for case 2 is displayed in Figure 4.18. The only significant difference in the lift coefficient between case 1 and case 2 is the decrease near the blade tip. Otherwise the values are nearly the same in both cases.

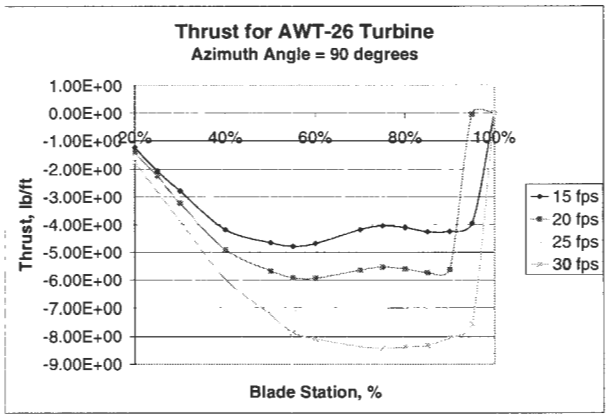

Figure 4.16 Thrust for Rot3dc Case 2

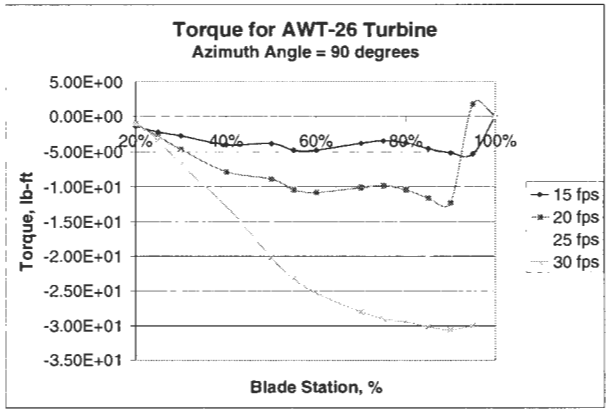

Figure 4.17 Torque Force for Rot3dc Case 2

The drag coefficient is shown in Figure 4.19. Similar to the total drag, the drag coefficient is somewhat higher for this case than for the rotor-only case. Radial velocity for case 2 is shown in Figure 4.20. No significant change is noted between cases 1 and 2 for this particular characteristic.

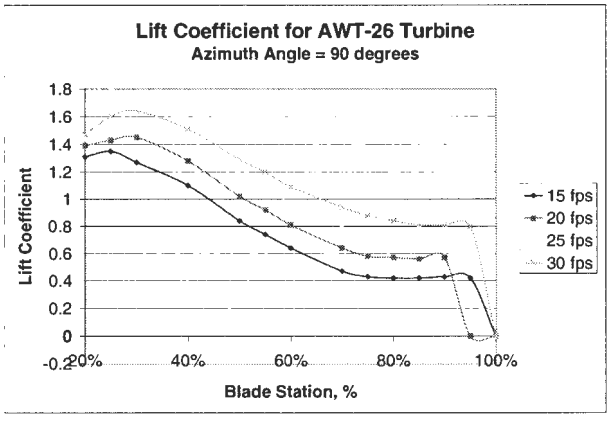

Figure 4.18 Lift Coefficient for Rot3dc Case 2

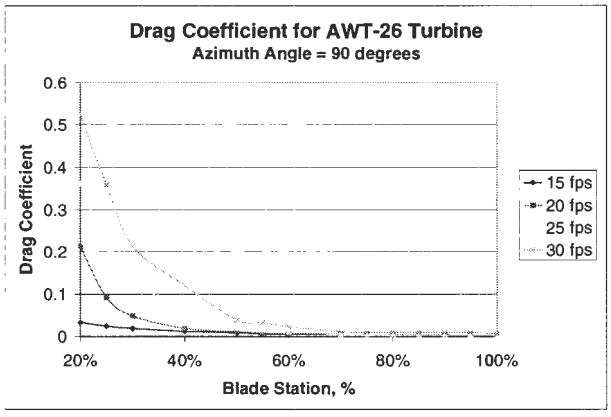

Figure 4.19 Drag Coefficient for Rot3dc Case 2

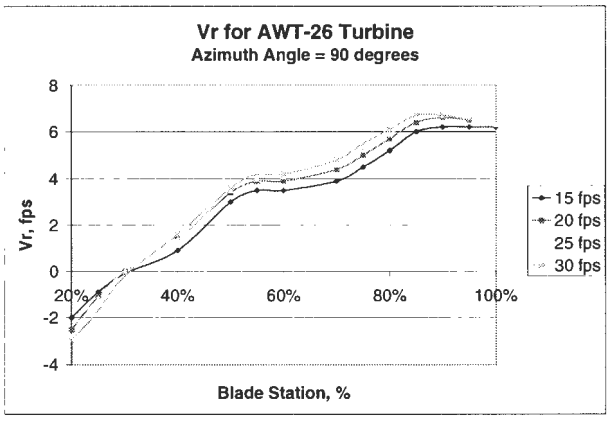

Figure 4.20 Radial Velocity for Rot3dc Case 2

Angular velocity for case 2 is shown in Figure 4.21. This graph is significantly different from the angular velocity for case 1. Further analysis is needed to determine the reason behind this dramatic change. Velocity in the direction of the freestream velocity and perpendicular to the plane of the rotor is shown in Figure 4.22. A slight increase can be seen in this case compared to case 1, but the general shape of the curves is the same.

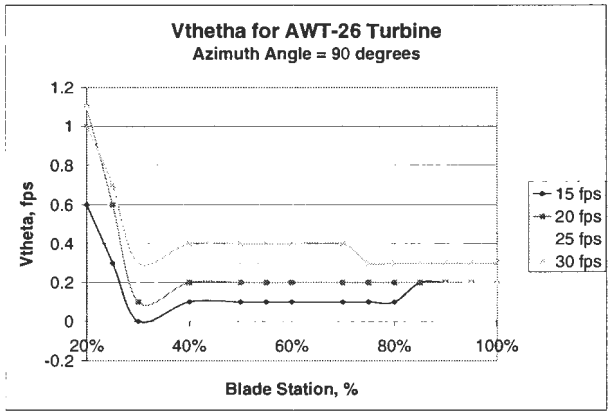

Figure 4.21 Angular Velocity for Rot3dc Case 2

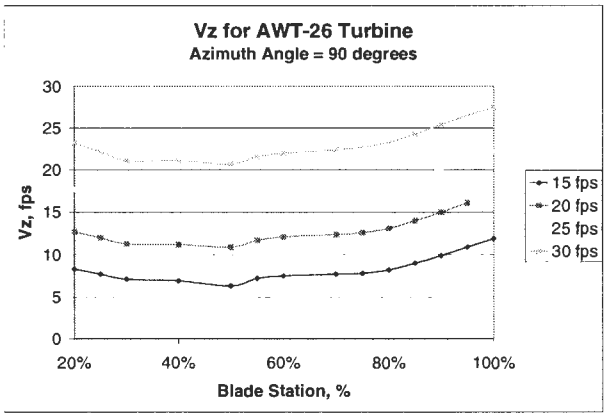

Figure 4.22 Axial Velocity for Rot3dc Case 2

4.5.3 Rot3dc Case 3: Single turbine on small sloping terrain

In this case, a sloping terrain was added to the model. The terrain was 60 feet by 60 feet with a 12 foot height at the center. The turbine was placed at the highest point of the terrain. The same wind speeds were used in this case. A diagram of the system is shown in Figure 4.23, and the results are shown in Figures 4.24 to 4.33.

The blade element results are provided for an azimuth angle of 90 degrees. Figure 4.24 shows the angle of attack profile for case 3. The addition of the small sloping terrain has caused the angle of attack to decrease and more closely match the angle of attack profile for the rotor-only case.

Figures 4.25 and 4.26 show the lift and load for case 3. These values are almost identical to cases 1 and 2, so apparently the nacelle, tower, and terrain have a negligible effect on these blade element characteristics. Drag for case 3 is illustrated in Figure 4.27. Compared to cases 1 and 2, drag is somewhat lower with the addition of the small sloping terrain.

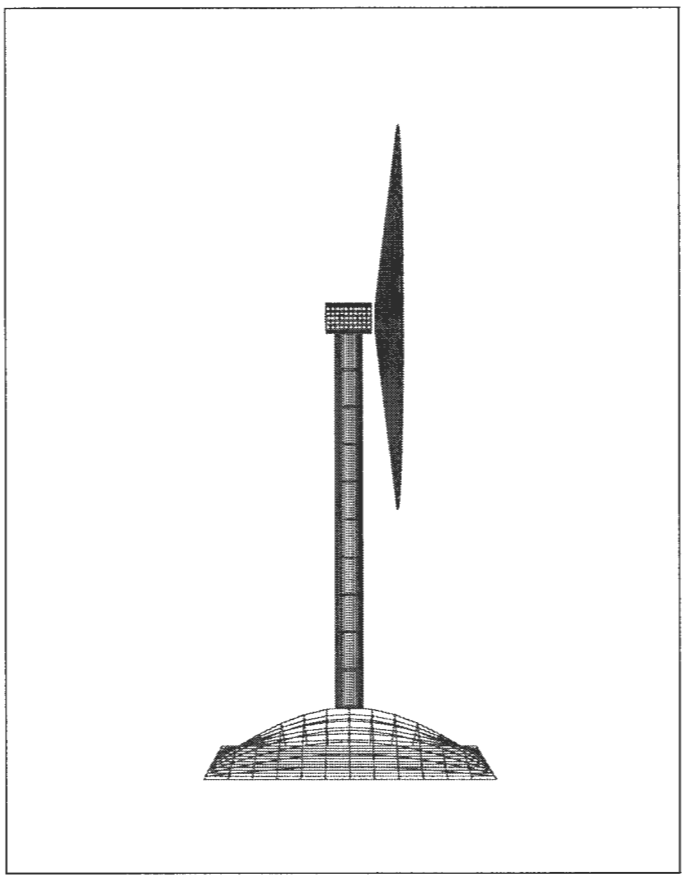

Figure 4.23 Model of AWT-26 Turbine on Small Sloping Terrain

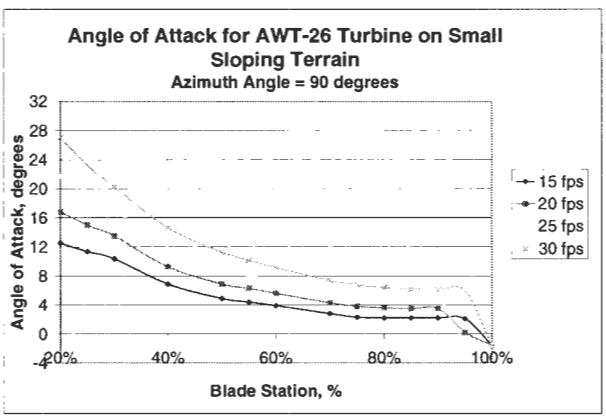

Figure 4.24 Angle of Attack for Rot3dc Case 3

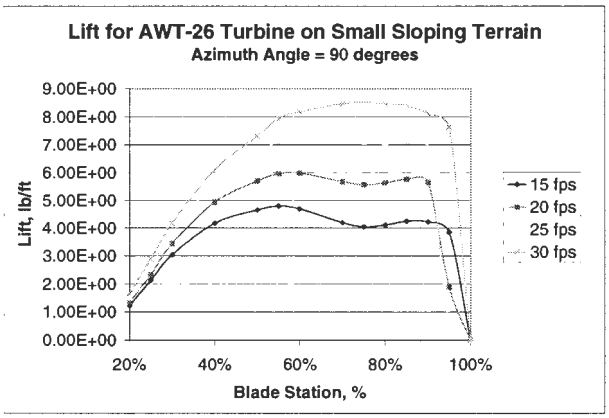

Figure 4.25 Lift for Rot3dc Case 3

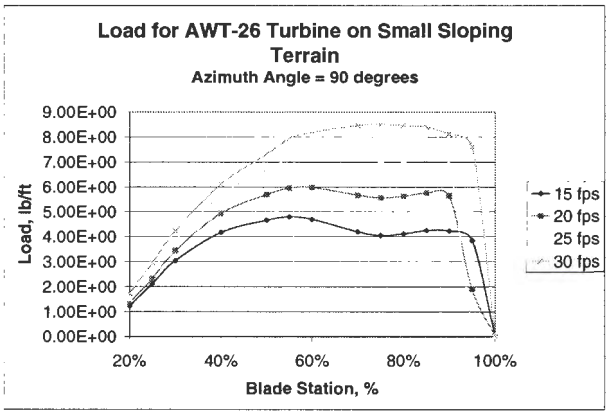

Figure 4.26 Load for Rot3dc Case 3

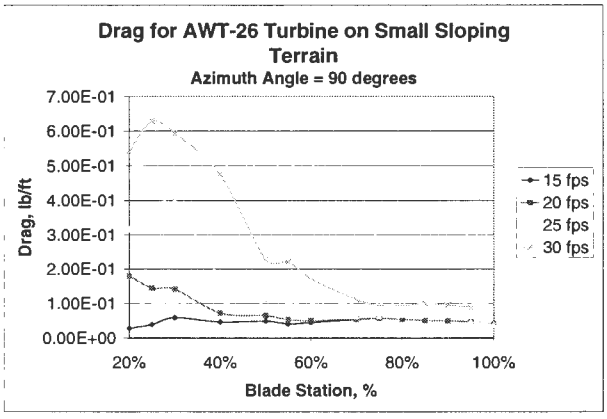

Figure 4.27 Drag for Rot3dc Case 3

Similar to lift and load, thrust and torque force, shown in Figures 4.28 and 4.29, show no significant differences in case 3. Since lift showed no significant change, the lift coefficient is not expected to display any change. The only noticeable variation is the slightly higher coefficient between the 20% and 30% blade stations. This can be seen in Figure 4.30.

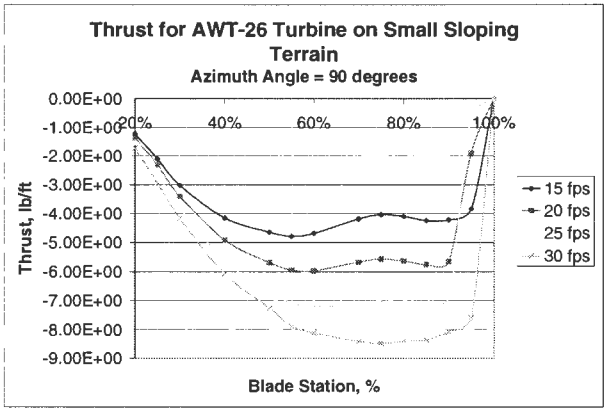

Figure 4.28 Thrust for Rot3dc Case 3

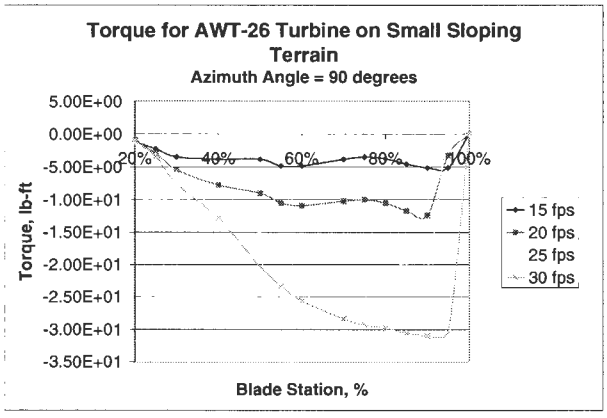

Figure 4.29 Torque Force for Rot3dc Case 3

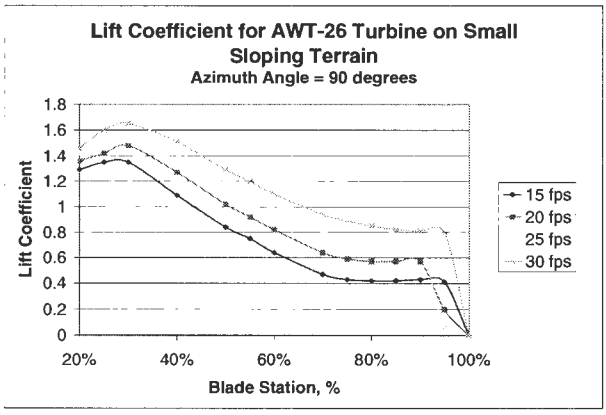

Figure 4.30 Lift Coefficient for Rot3dc Case 3

Since drag experienced some changes between cases 1 and 3, so did the drag coefficient, shown in Figure 4.31. It decreased from case 2, and more closely resembles the drag coefficient profile for case 1. Figure 4.32 illustrates the radial velocity for case 3. One can see a slight, but noticeable increase over cases 1 and 2. The shape of the curves are similar to the previous cases.

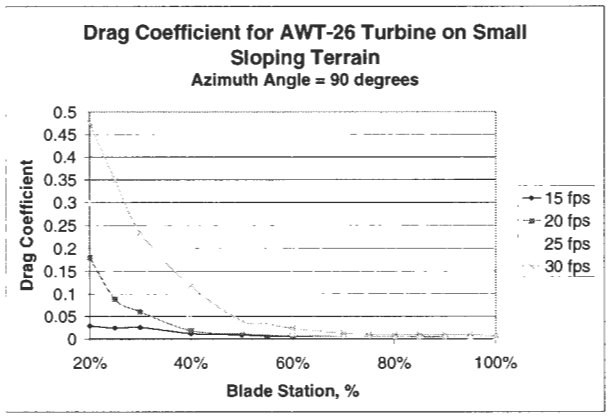

Figure 4.31 Drag Coefficient for Rot3dc Case 3

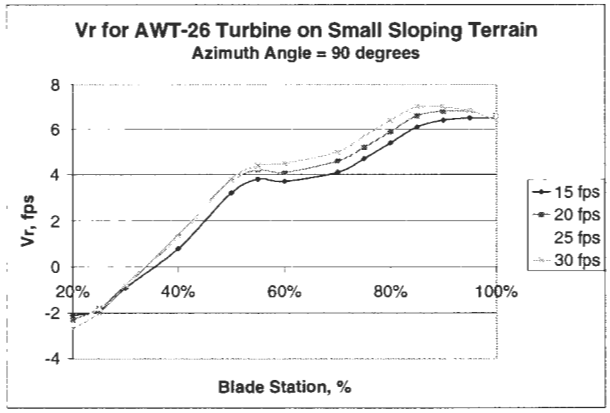

Figure 4.32 Radial Velocity for Rot3dc Case 3

Figure 4.33 portrays the angular velocity for the AWT-26 turbine on a small sloping terrain. Unlike case 1, the angular velocity never reaches zero for any of the wind speeds, and the shape of the curves differ significantly. Figure 4.34 depicts the velocity of the flow perpendicular to the rotor for case 3. No significant change is noted between this case and the previous two cases.

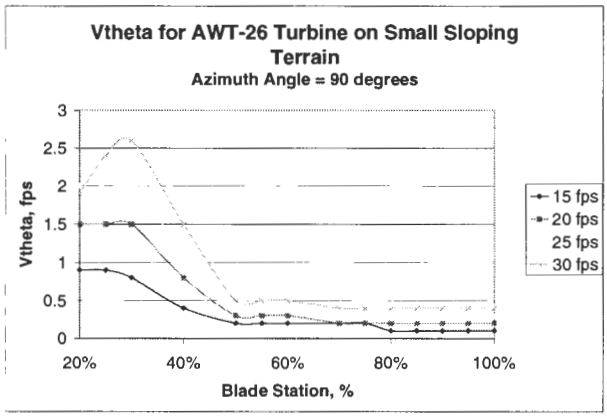

Figure 4.33 Angular Velocity for Rot3dc Case 3

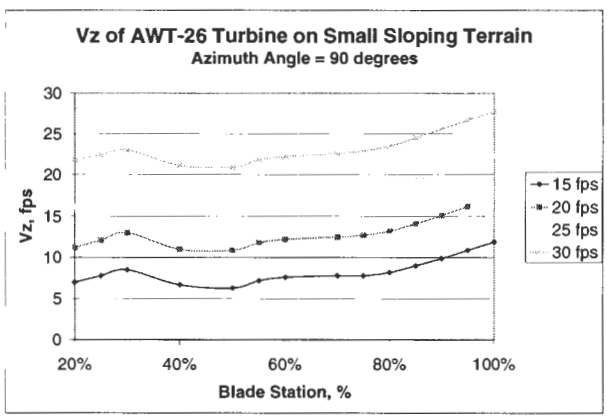

Figure 4.34 Axial Velocity for Rot3dc Case 3

4.5.4 Rot3dc Case 4: Single turbine on large sloping terrain

A larger terrain was included in this case, 120 by 120 feet with a 24 foot height at the center. The turbine was placed at the center of the terrain. This case was run at wind speed of 20 feet per second.

Figure 4.35 shows the angle of attack for case 4. The figure shows negligible differences between the large and small terrain cases.

Figures 4.36 and 4.37 show the lift and drag coefficients for case 4. Similar to the angle of attack, the lift and drag coefficient profiles for the large sloping terrain are nearly identical. Apparently the larger terrain has a negligible influence on the flow through the rotor.

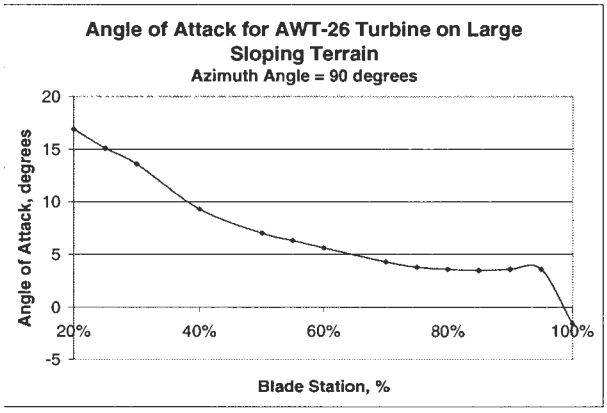

Figure 4.35 Angle of Attack for Rot3dc Case 4

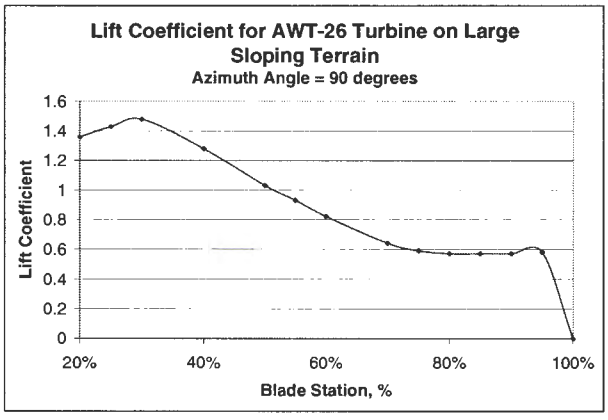

Figure 4.36 Lift Coefficient for Rot3dc Case 4

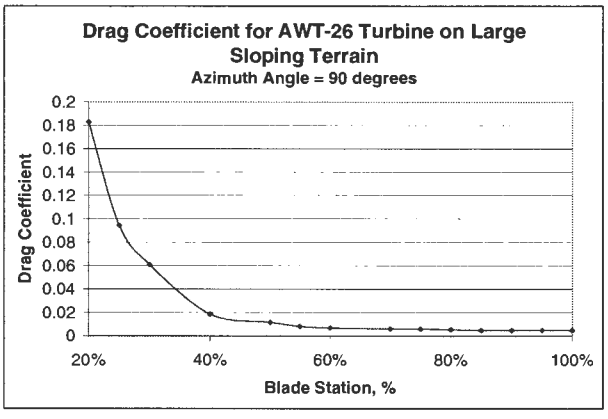

Figure 4.37 Drag Coefficient for Rot3dc Case 4

4.5.5 Rot3dc Case 5: Single turbine offset on large sloping terrain

Another capability of the Rot3dc program is the ability to model turbines at any point on a terrain. In this case, the turbine was placed half way between the center and end of the terrain. This case was also run at a wind speed of 20 feet per second.

Figure 4.38 shows the angle of attack for case 5. Apparently, the effect of the larger terrain size and the off-center location of the turbine was negligible compared to previous cases. Similarly, the lift and drag coefficients, shown in Figures 4.39 and 4.40, experience negligible change in case 5. Rot3dc has the capability of simulating two wind turbines, however, that option was not exercised for this thesis.

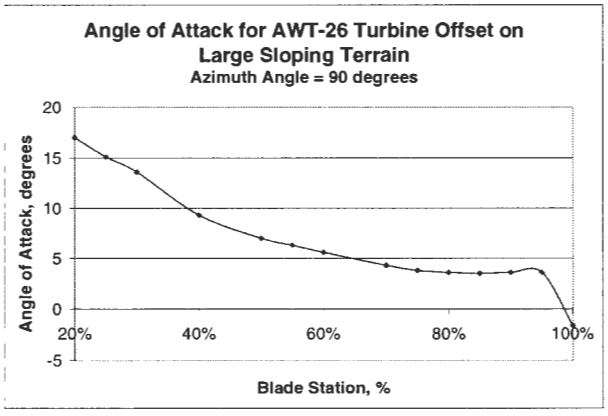

Figure 4.38 Angle of Attack for Rot3dc Case 5

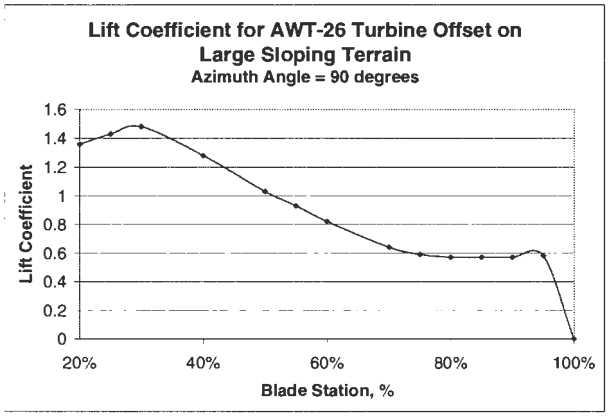

Figure 4.39 Lift Coefficient for Rot3dc Case 5

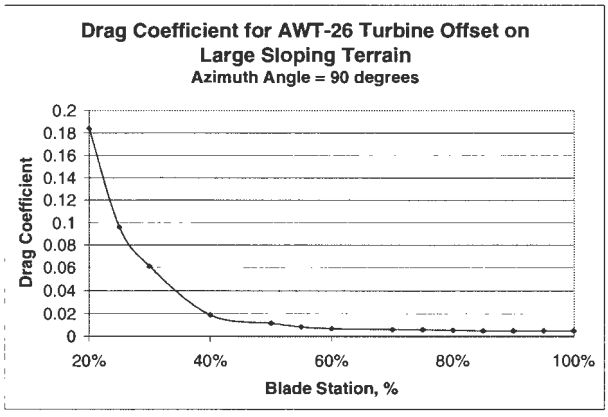

Figure 4.40 Drag Coefficient for Rot3dc Case 5

Figures 4.41 to 4.45 compare all five cases at a wind speed of 20 feet per second. As one can see from the charts, this method produces distinguishable differences between various wind turbine configurations, particularly near the blade tip which is the root cause of failures. This capability is unlike that of any other technique in use today.

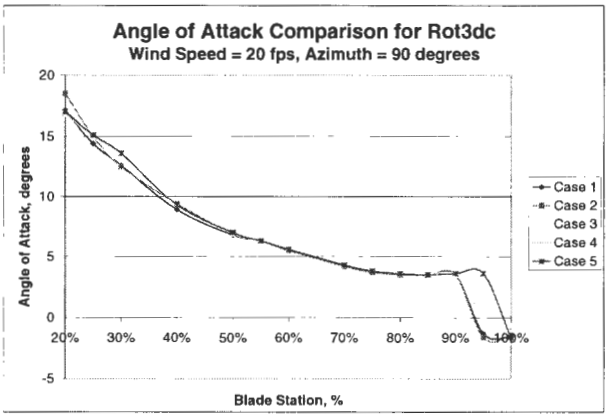

Figure 4.41 Angle of Attack Comparison for Cases 1 through 5

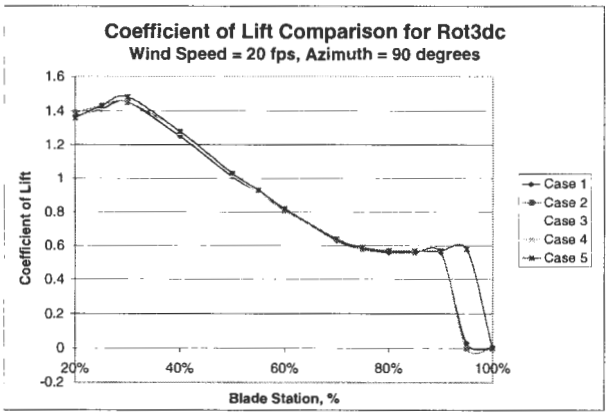

Figure 4.42 Coefficient of Lift Comparison for Cases 1 through 5

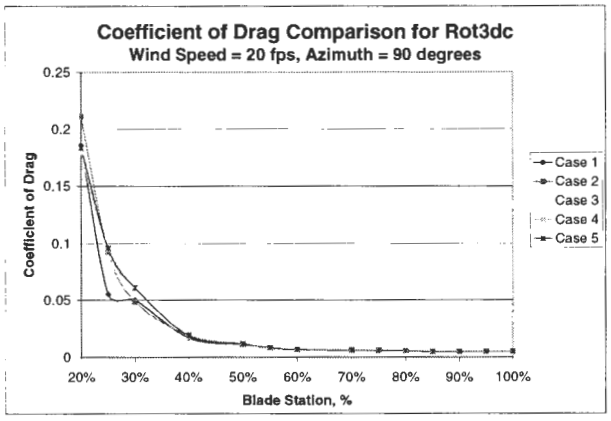

Figure 4.43 Coefficient of Drag Comparison for Cases 1 through 5

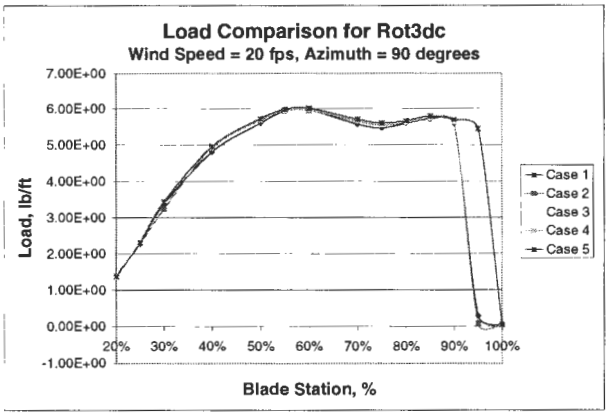

Figure 4.44 Load Comparison for Cases 1 through 5

4.6 Advanced Analysis

In the previous section it was shown that one can utilize the output from Rot3dc to analyze the variation of load, thrust, and other parameters along the length of the blade for a particular azimuth angle and at various wind speeds. More advanced analyses can also be performed. For instance, one can look at the cyclic variation of load. As the rotor blades rotate, they experience different loads. In the tower wake, the blades experience a dramatic change in loading. This sharp contrast in loading as the blades rotate contributes to fatigue and blade failure. Figure 4.45 shows an example of this phenomenon. At azimuth angles 90 and 270 degrees, to the left and right of the rotor respectively, the curves are virtually the same, except near the tip. At an azimuth angle of 180 degrees, however, where the blade passes through the tower's wake, the load decreases significantly. This fluctuation is high enough to cause vibrations that may ultimately reduce the lifetime of the blades.

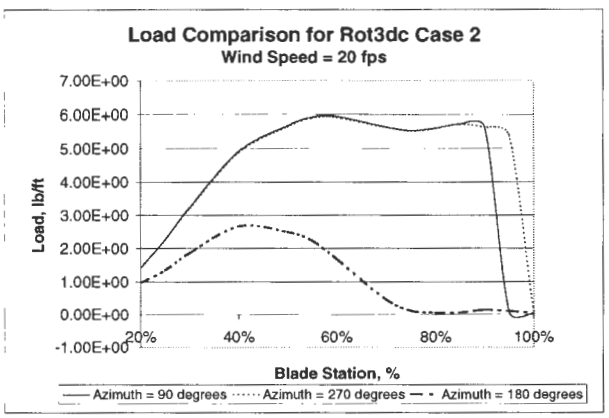

Figure 4.45 Load Comparison for Various Azimuth Angles

Figures 4.46 and 4.47 show similar results for thrust and torque along the length of the blade. In contrast, one can pick a location on the blade and analyze the cyclic load variation at that point. An example is shown in Figure 4.48. The blade tip, the part of the blade that is most sensitive to load variations, experiences a dramatic shift in load as it passes through the tower wake. All of these analyses are extremely useful in designing more durable rotor blades.

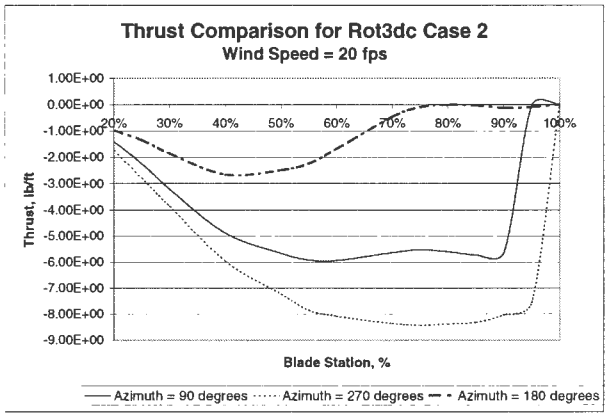

Figure 4.46 Thrust Comparison for Various Azimuth Angles

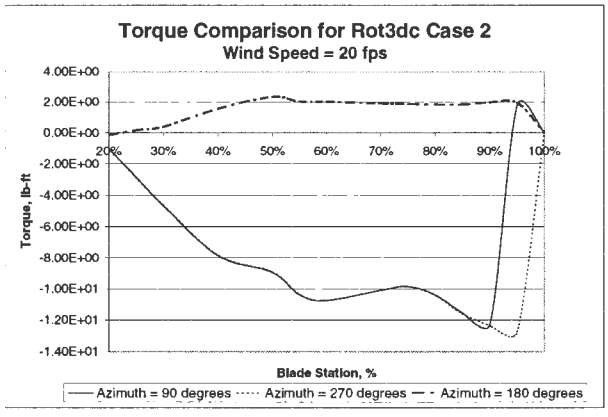

Figure 4.47 Torque Comparison for Various Azimuth Angles

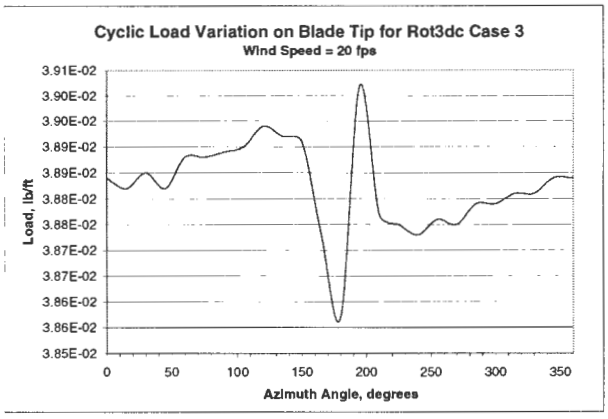

Figure 4.48 Cyclic Load Variation on Blade Tip for Rot3dc Case 3

4.7 Visualization

Rot3dc outputs flow visualization data formatted for a software package called FAST, Flow Analysis Software Toolkit, developed by members of the Numerical Aerodynamic Simulation Division at NASA Ames Research Center in California. This package gives the user a variety of tools to visualize the flow solution. Some of these solutions include pressure, momentum, density, energy, enthalpy, velocity, vorticity, swirl, among others. They can be visualized on a variety of two-dimensional planes. FAST also gives the user the option of using the planes provided by the Cartesian grid of the computational domain or other planes. It is a very versatile tool. An example of the flow visualization is shown in Figures 4.40, 4.41, and 4.42.

Figure 4.41 shows the velocity profile in a plane parallel to the freestream velocity for Rot3dc case 3. The vectors show the flow field, with the influence of the rotor, the tower, and the terrain displayed. The vectors show how the rotor extracts energy from the flow, resulting in a decrease in flow velocity. This diagram also demonstrates that the tower has a more significant impact on the flow through the rotor than does the terrain.

Figure 4.42 shows the vorticity profile for Rot3dc case 3. Vorticity is created by the rotational motion of the wind turbine blades. The freestream has no vorticity; vorticity is

induced by the rotation of the blades. Maximum vorticity can be seen near the center of the rotor, as would be expected. Vorticity is also introduced in the wake of the tower and the terrain.

Figure 4.43 displays the pressure contour profile for Rot3dc case 3. The greatest pressure is felt at the leading edge of the tower and the rotor blades. Pressure varies along the length of the blades, with the sharpest gradients near the blade tip. This uneven pressure distribution affects the lifetime of the blades by causing stress and fatigue.

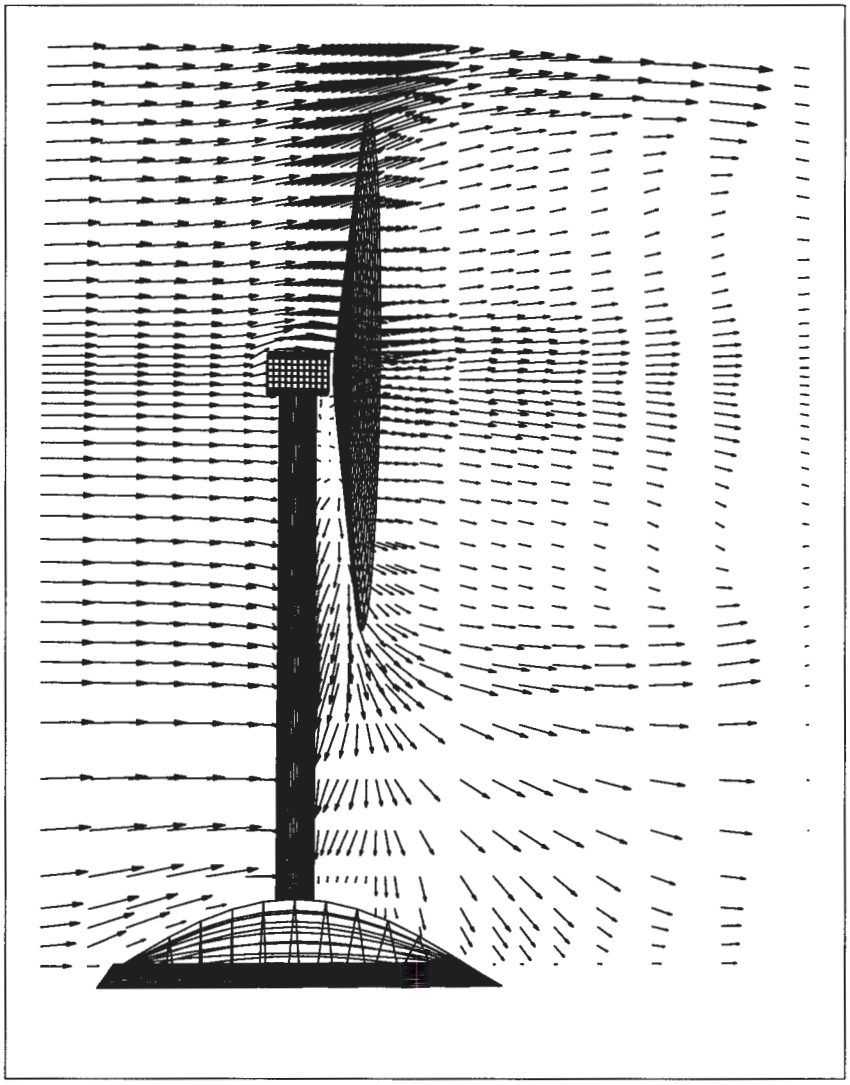

Figure 4.49 Velocity Profile for AWT-26 Turbine on Small Sloping Terrain for Wind Speed of 20 fps

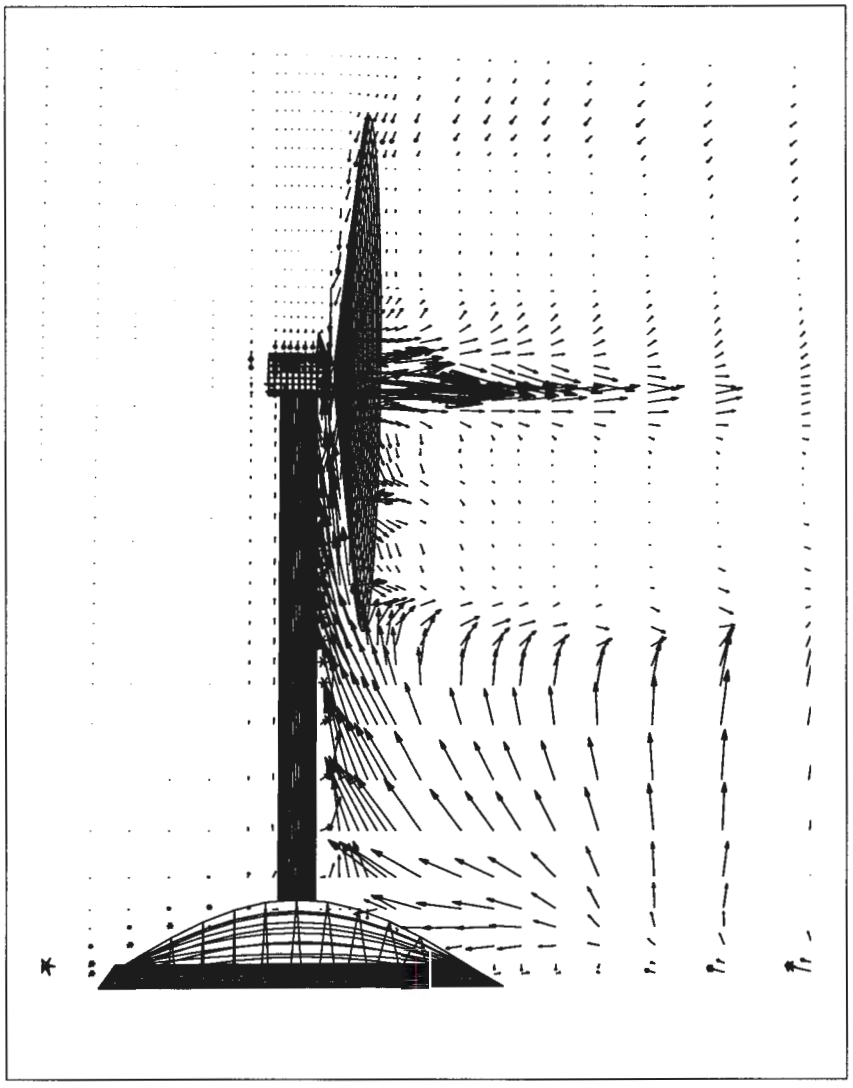

Figure 4.50 Vorticity Profile for AWT-26 Turbine on Small Sloping Terrain for Wind Speed of 20 fps

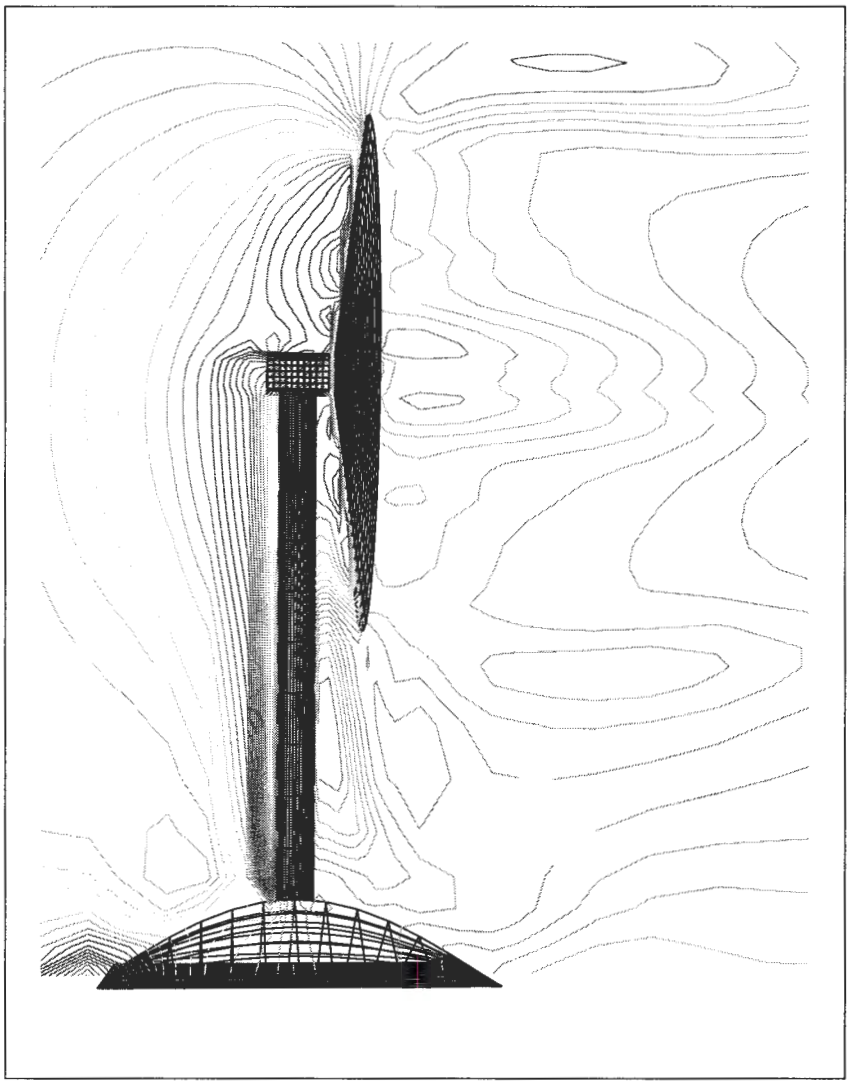

Figure 4.51 Pressure Profile for AWT-26 Turbine on Small Sloping Terrain for Wind Speed of 20 fps

CHAPTER 5. COMPARISON TO WT_PERF

5.1 Introduction

WT_Perf is a wind turbine performance computer program developed by the National Renewable Energy Laboratory. It was derived from Aerovironment's PROP code, which was based upon work done by Robert Wilson and Stel Walker at Oregon State University. There is no documentation for this code, but it has been used by the wind turbine industry to design and analyze wind turbines (Buhl et al. 2).

The algorithms in WT_Perf are based upon the Glauert Momentum strip theory. In this theory, the momentum of the air going through an annular strip described by the rotor blades is equated with blade forces found from two-dimensional airfoil theory. Axial and circumferential interference factors are then computed from this change in momentum. Prandtl tip-loss and hub-loss corrections are included to increase accuracy (Buhl).

A test case was run in WT_Perf as a comparison to Rot3dc. Up to now, only codes such as WT_Perf have been availabe for the design of wind turbines. These codes have several limitations that minimize the effectiveness of their use. By comparing the output of Rot3dc to WT_Perf, one can see that Rot3dc offers a more realistic performance profile, as well as more information that has not been available through previous computer codes.

5.2 Description of Test Case

The AWT-26 wind turbine was modeled in WT_Perf for wind speeds of 10 to 35 fps. The same airfoil table and chord/twist table was used for both the Rot3dc and WT_Perf cases. The results are shown in the Figures 5.1 to 5.3.

The angle of attack profiles shown in Figure 5.1 appear consistent with theory, in that they increase as wind speed increases, and they decrease as one goes along the length of the blade. The general shape of the curves is consistent with that of Rot3dc, except that the angle of attack does not go to zero at the tip. In actuality, the angle of attack should go to zero at the tip. The fact that it does not in the WT_Perf case shows the limitations of this program.

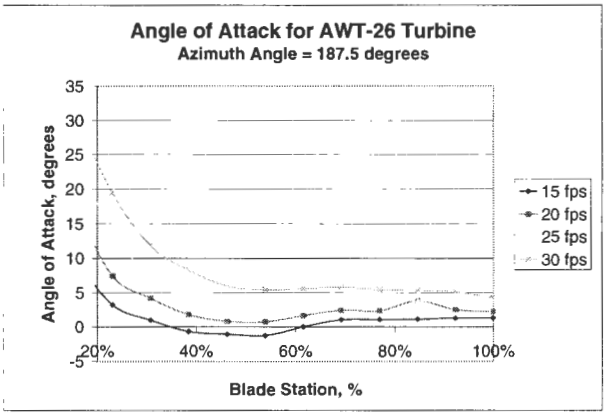

Figure 5.1 Angle of Attack for WT_Perf Case

The lift coefficient profiles displayed in Figure 5.2 has a similar shape to that of Rot3dc; however, the values are somewhat lower. An error in the output also seems to be present at the 85% blade station for the 20 fps case. Similar to the angle of attack, the values do not go to zero at the blade tip as done in Rot3dc.

The drag coefficient for WT_Perf is represented in Figure 5.3. It has a similar shape to that for Rot3dc, and the initial values are virtually the same. However, the drag coefficient appears to drop to negligible levels at the 35% blade station, whereas in the Rot3dc case, this happens at the 70% blade station.

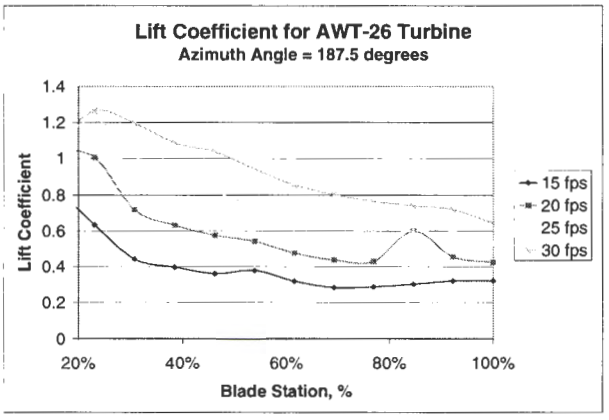

Figure 5.2 Lift Coefficient for WT_Perf Case

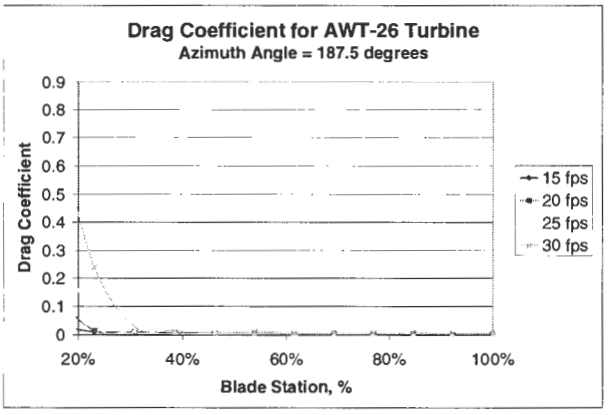

Figure 5.3 Drag Coefficient for WT_Perf Case

5.3 Comparison

WT_Perf appears to compute high power coefficients at high wind speeds and low power coefficients at low wind speeds compared to Rot3dc, as can be seen by Figure 5.4. This is probably the case because WT_Perf does not actually model the effects of the influence of the nacelle and tower on the flow. For this reaston, WT_Perf tends to present an overly-optimistic performance for wind turbines. Figure 5.5 shows the power coefficient with respect to tip speed ratio, a function of wind speed, given by equation 2.10 in Chapter 2.

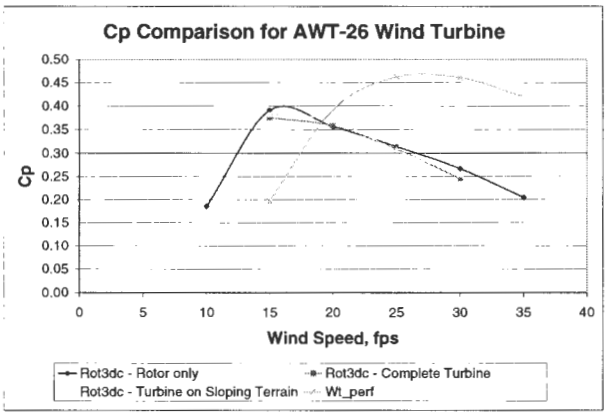

Figure 5.4 Comparison of Power Coefficient for WT_Perf and Rot3dc Cases

Comparison of the angles of attack and coefficients of lift and drag are presented in Figures 5.6, 5.7, and 5.8 for a wind speed of 20 fps, where the power coefficients for Rot3dc and WT_Perf were closest in magnitude. The azimuth angles did not match up exactly between the two codes; therefore, the WT_Perf results are presented for an azimuth angle of 187.5 degrees, while that of Rot3dc are for an azimuth angle of 180 degrees. The general shape of the curves in each case is similar, however they do not match exactly. WT_Perf underpredicts Rot3dc in all cases.

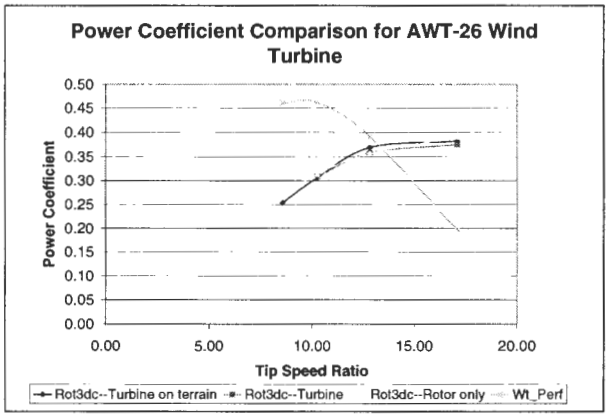

Figure 5.5 Comparison of Power Coefficient for WT_Perf and Rot3dc Cases

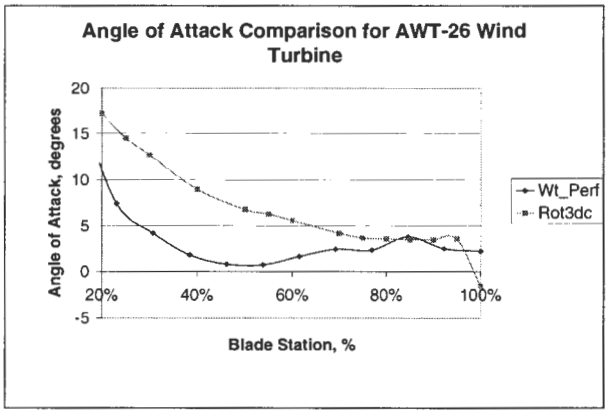

Figure 5.6 Comparison of Angle of Attack for WT_Perf and Rot3dc Cases at Wind Speed of 20 fps

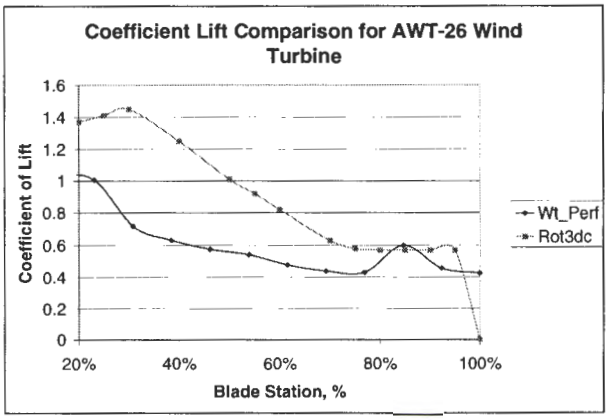

Figure 5.7 Comparison of Lift Coefficient for WT_Perf and Rot3dc Cases at Wind Speed of 20 fps

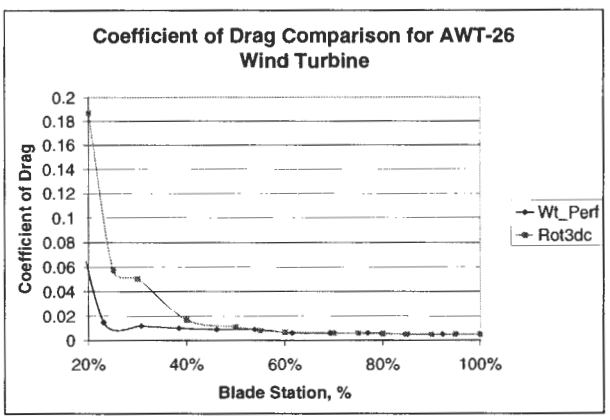

Figure 5.8 Comparison of Coefficient of Drag for WT_Perf and Rot3dc Cases at Wind Speed of 20 fps

CHAPTER 6. CONCLUSIONS

The goal of this research was to utilize a computational fluid dynamics program, called Rot3dc, to simulate and analyze wind turbine performance in a realistic environment. This research also intended to compare the results of this simulation to WT_Perf, a simplistic computer code developed in the 1970s that was designed to calculate wind turbine performance using Glauert Momentum strip theory.

First, a description of the procedure was provided. The flow field was modeled by numerical solution to the Navier-Stokes equations. The rotor was modeled as momentum sources in the equations that govern the flow. The computational domain was specified as a rectangular parallelpiped with several layers and the turbine at the center. A discussion of the output generated by the program was provided.

This research ran several test cases, including a single turbine rotor, a complete turbine with nacelle and tower on a flat terrain, a complete turbine on a small sloping terrain, a complete turbine on a large sloping terrain, and a complete turbine offset from the center of a large sloping terrain. For each case, the CFD program produced data on angle of attack, lift, drag, thrust, and torque along the length of the blade as well as at various points as it makes a complete rotation. It also generated the various components of flow velocity and the coefficient of power at each wind speed. Furthermore, it provided flow field solutions that could be visualized in FAST, Flow Analysis Software Toolkit. This information is extremely useful in designing rotors that minimize variations in loading, bending, and twisting that cause fatigue and reduce the life of the blades.

Compared to WT_Perf, a computer code currently in use by industry and the scientific community, this research showed that CFD is a more versatile tool. The CFD program is

able to model the influence on the flow by solid bodies, such as a nacelle, tower, and terrain, whereas WT_Perf merely applies loss factors for these items. This capability allows for advanced analyses of the cyclic variation of load on the rotor blades, the load distribution along the length of the blade, and other characteristics that cause fatigue and failure of the blades; no traditional approach can do that. The CFD method produces results that show differences between the different wind turbine configurations. Computer codes currently in use cannot make this distinction.

Rot3dc also has the capability to model the influence of two turbines; however, this component was not exercised in this study. Overall, CFD provides analysis in more realistic wind turbine environments, rather than idealistic environments.

In addition to the level of sophistication CFD provides, another advantage includes its user-friendly windows-based environment. This environment makes it easy to load new models in a short time and to make changes when needed.

As one can see, CFD can have a significant impact on the wind turbine industry. Up to now, no tool has been available that could provide the level of analysis that CFD can. With this new technique, rotors can be designed to minimize fatigue, increasing the lifetime of the blades, improving the performance of the rotor, and ultimately reducing the overall cost. Reduced costs will help make wind power more competitive with fossil fuels.

While CFD has many advantages, it does have some drawbacks—Rot3dc requires significant computer memory and computation time. For this study, Silicon Graphics O_2 computers were used, and each run required 100 iterations to converge. To obtain this level of convergence, each run took between 30 and 35 hours to complete and utilized approximately 24 megabytes of memory and about 15 megabytes of storage space. Compared to traditional programs like WT_Perf, which runs in just a few seconds and uses 1 megabyte of storage space, these requirements may seem impractical for regular use. Although the windows-based environment of Rot3dc is user-friendly, it still requires advanced understanding of the input values and output results. It also requires significant post-processing and analysis of the output in order for the information to be useful.

6.1 Recommendations for Further Study

This research provides an overview of the capabilities of CFD as a more sophisticated method of simulating wind turbine performance; however, more study is needed. For instance, more work is needed to accurately model the nacelle, tower, and terrain. In this study, the tower was modeled as a simplistic cylindrical tube with constant diameter. Typically, however, the diameter of the tower base is larger than at the top. Also, nacelles are often designed to be more aerodynamic than a rectangular box. These modifications could provide more accurate results.

A variety of terrains could also be modeled in further studies. In fact, geography from actual sites could be used to simulate a more realistic environment than what was used in this study. With a more realistic terrain, turbines could be positioned at a variety of locations to determine the optimal placement. This capability could have a dramatic impact on the development of wind turbine sites.

The two turbine case could be run to analyze the interference effects of multiple turbines in a realistic environment. And finally, this data should be compared to field test data to assess its accuracy to a real environment. In this study, field test data was requested, but since it is proprietary data, none was available for use. Although this method has been verified in helicopter applications, it should be validated for wind turbines before widespread use.

BIBLIOGRAPHY

Buhl, Marshall. "Prop-PC." *NWTC Design Codes*. [Web page]. Golden: National Wind Technology Center, 1998. Available: http://wind2.nrel.gov/designcodes/proppc/ [June 6, 1999].

Buhl, M. L., A. D. Wright, and J. L. Tangler. "Wind Turbine Design Codes: A Preliminary Comparison of the Aerodynamics." Golden: National Renewable Energy Laboratory, 1997.

Cavallo, Alfred J., Susan M. Hock, and Don R. Smith. "Wind Energy: Technology and Economics." *Renewable Energy: Sources for Fuels and Electricity. Renewable Energy: Sources for Fuels and Electricity.* Ed. Thomas B. Johansson et al. Washington DC: Island Press, 1993. 121-156.

Eggleston, David M. and Forrest S. Stoddard. *Wind Turbine Engineering Design*. New York: Van Nostrand Reinhold, 1987.

Elliott, D. L., ed. *Wind Energy Resource Atlas of the United States*. Golden: Solar Technical Information Program and Solar Energy Research Institute, 1987.

Johansson, Thomas B., Henry Kelly, Amulya K. N. Reddy, and Robert H. Williams, eds. *Renewable Energy: Sources for Fuels and Electricity*. Washington DC: Island Press, 1993.

Leslie, Jennifer A. "Methanol Production from Combined Biomass and Wind Resources in North Dakota." Senior thesis, Princeton U, 1993.

Mathur, Sanjay R. "Three Dimensional Analysis of a Rotor in Forward Flight." Master's thesis, Iowa State U, 1989.

Patankar, S. V. "Numerical Heat Transfer and Fluid Flow." Washington DC: McGraw-Hill, 1980.

Rajagopalan, R. G., D. E. Berg, and P. C. Klimas. "Development of a Three-Dimensional Model for the Darrius Rotor and Its Wake." *Journal of Propulstion and Power* 11.2 (1995): 185–195.

Rajagopalan, R. Ganesh and Sanjay R. Mathur. "Three Dimensional Analysis of a Rotor in Forward Flight." *Journal of the American Helicopter Society* July 1993: 14–25.

Rot3dc: Rotor Modeling Simulation Package with Graphical User Interface. Ames: Sukra Helitek Inc, 1998.

Spera, David A., ed. *Wind Turbine Technology: Fundamental Concepts of Wind Turbine Engineering*. New York: ASME Press, 1994.

Walker, John F. and Nicholas Jenkins. *Wind Energy Technology*. New York: Wiley, 1997.

ACKNOWLEDGEMENTS

I would like to take this opportunity to express my appreciation to those who helped me with various aspects of conducting research and the writing of this thesis. First and foremost, Dr. R. Ganesh Rajagopalan for his guidance, patience and support throughout this research and the writing of this thesis.

I would also like to thank my committee members for their suggestions and contributions: Dr. Robert Brown and Dr. Ron Nelson. I would additionally like to thank Sukra Helitek, Inc. for their permission to use Rot3dc and for their assistance in developing the various simulations performed in this research. Thanks also go to Marshall Buhl from the National Wind Technology Center for his assistance with WT_Perf.